AR-40/AR-39 AGE STUDIES OF MAFIC VOLCANICS FROM THE SVERDRUP BASIN, ARCTIC CANADA

BY

HEATHER A. AVISON

SUBMITTED IN PARTIAL FULFILLMENT OF THE REQUIREMENTS

FOR THE DEGREE OF BACHELOR OF SCIENCE, HONOURS

AT

DALHOUSIE UNIVERSITY

HALIFAX, NOVA SCOTIA

MARCH, 1987

DALHOUSIE UNIVERSITY
Department of Geology
Halifax, N.S. Canada B3H 3J5 Telephone (902) 424-2358 Telex:019-21863

DALHOUSIE UNIVERSITY, DEPARTMENT OF GEOLOGY

B.Sc. HONOURS THESIS

Author: HEATHER A. AVISON

Title: AR-40/AR-39 AGE STUDIES OF MAFIC VOLCANICS FROM THE SVERDRUP BASIN, ARCTIC CANADA

Date: April 24, 1987

Distribution License

DalSpace requires agreement to this non-exclusive distribution license before your item can appear on DalSpace.

NON-EXCLUSIVE DISTRIBUTION LICENSE

You (the author(s) or copyright owner) grant to Dalhousie University the non-exclusive right to reproduce and distribute your submission worldwide in any medium.

You agree that Dalhousie University may, without changing the content, reformat the submission for the purpose of preservation.

You also agree that Dalhousie University may keep more than one copy of this submission for purposes of security, back-up and preservation.

You agree that the submission is your original work, and that you have the right to grant the rights contained in this license. You also agree that your submission does not, to the best of your knowledge, infringe upon anyone's copyright.

If the submission contains material for which you do not hold copyright, you agree that you have obtained the unrestricted permission of the copyright owner to grant Dalhousie University the rights required by this license, and that such third-party owned material is clearly identified and acknowledged within the text or content of the submission.

If the submission is based upon work that has been sponsored or supported by an agency or organization other than Dalhousie University, you assert that you have fulfilled any right of review or other obligations required by such contract or agreement.

Dalhousie University will clearly identify your name(s) as the author(s) or owner(s) of the submission, and will not make any alteration to the content of the files that you have submitted.

If you have questions regarding this license please contact the repository manager at dalspace@dal.ca.

Grant the distribution license by signing and dating below.

_____ _____

Name of signatory Date

Abstract

Cretaceous extrusive volcanism in the Sverdrup Basin is widespread and appears to have occurred in four major episodes (Valanginian, late Barremian, late Albian, and late Cenomanian/early Turonian). In addition to these flows, the basin is cut by abundant dykes and sills which have been dated by various researchers to range from Jurassic to Upper Cretaceous in age. Some correlation between the intrusive and extrusive activity may be expected, and therefore the reliability of the intrusive ages has been questioned.

Ar-40/Ar-39 step-heating analyses have been carried out on 10 fractions from four igneous bodies in the Sverdrup Basin. The rock samples were chosen so that in addition to discovering the ages of the units sampled, the rock components best suited for dating these mafic bodies could be determined.

The results of this study show that high-K deuteric phases from body interiors and chilled margin samples containing high-K phases produce the most reliable ages; provided they have not experienced a subsequent thermal disturbance above their argon blocking temperatures (generally <200°C). It is also shown that low-K separates such as mafics or plagioclase yield unreliable ages, even when the samples are apparently undisturbed.

In every case, the age of the unit was found to coincide with one of the major extrusive volcanic episodes. A sill at Buchanan Lake, Axel Heiberg Island, yields an age of 126±2 Ma, and was apparently emplaced during the Valanginian episode. A dyke which cross-cuts this sill was dated to be 113±6 Ma, concurrent with volcanics of the Barremian episode outcropping at Camp Five Creek near Bunde Fjord. Both a flow and a sill near Lake Hazen, Ellesmere Island, were apparently emplaced during the Turonian episode (92±2 Ma and 91±2 Ma, respectively). Flows from this fourth episode are also found near the basin margin at Hanson Point, northern Ellesmere Island.

Acknowledgements

First of all I wish to thank especially my supervisors, Dr. G.K. Muecke and Dr. P.H. Reynolds, for their support, guidance, and enthusiasm for this thesis. Thanks also go out to Marie-Claude Williamson who, along with Dr.Muecke, collected the samples from the Arctic.

In carrying out this research, I received a great deal of invaluable assistance from several others. These include Keith Taylor, Peter Elias, Sandy Grist, Bob McKay, Steve Dudka, Doug Merrett, and Scott Avison (who helped type "those wretched tables"!). I am truly indebted.

Table of Contents

List of Figures

List of Tables

Chapter 1. Introduction

The Sverdrup Basin in the Canadian Arctic islands is one of Canada's frontier hydrocarbon provinces. Although geological mapping and exploratory drilling have provided a considerable amount of information on the evolution of the basin, many aspects of its development still remain to be explored. This is particularly true for the large volume of extrusive and intrusive igneous rocks which are part of the basin.

Some of the work which has been carried out to date includes the dating of igneous sills, dykes, and flows, both stratigraphically and isotopically. The conventional K-Ar method of radiometric dating has been the most commonly used technique for the mafic intrusives in the area. The intrusive ages (derived by this method and others), show a wide spread, from, lower Jurassic to Upper Cretaceous (See figure 2 and table 1). The extrusives, which in many cases can be dated stratigraphically, fall into four distinct episodes in the Cretaceous. This excludes the much earlier Carboniferous and Permian flows (Embry, in prep.). It would seem reasonable to expect some degree of correlation between the episodes of intrusion and extrusion in the basin, so a question arises as to the reliability of the radiometric ages of the intrusives.

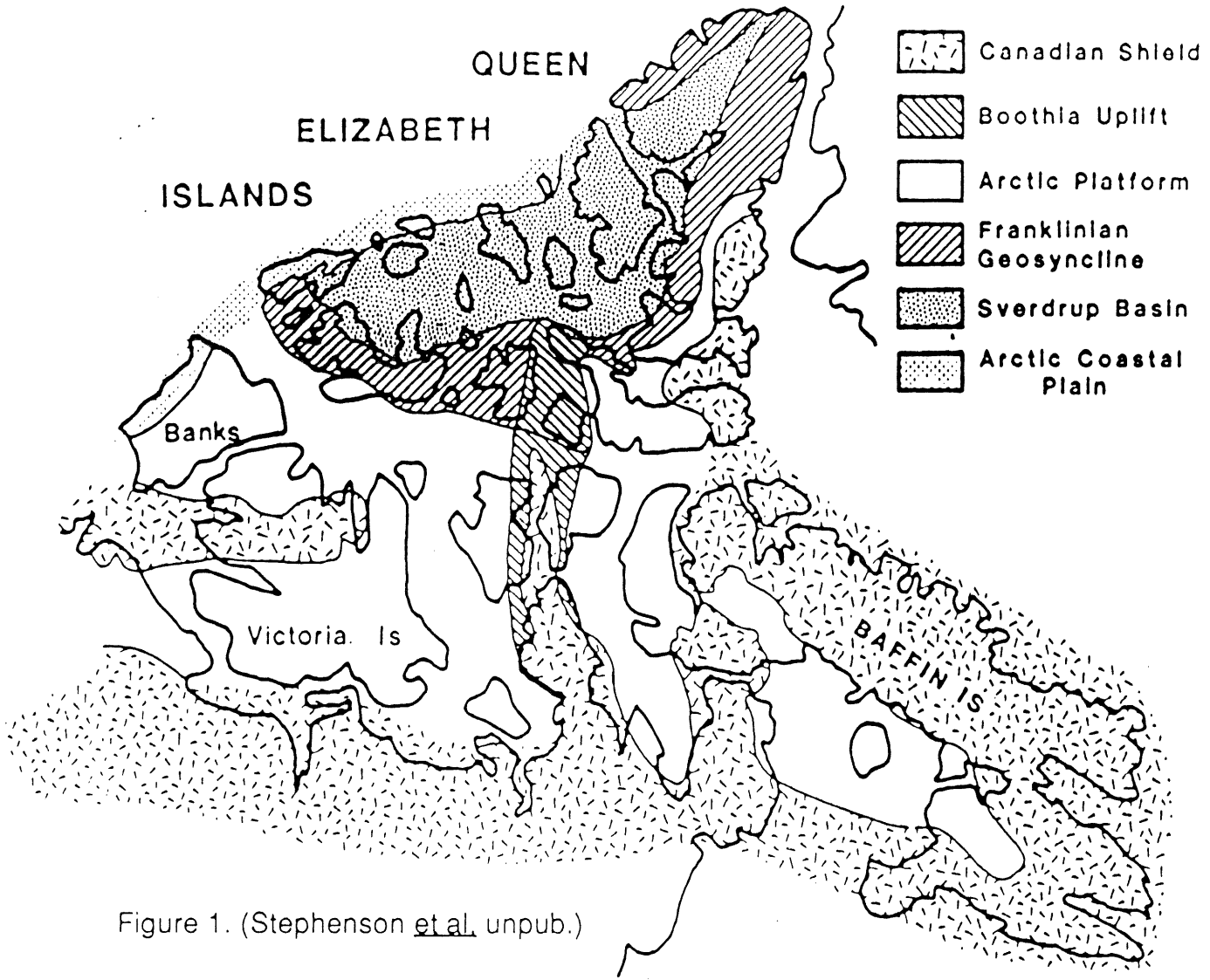

Figure 1. (Stephenson et al. unpub.)

after Thorsteinsson & Tozer, 1970

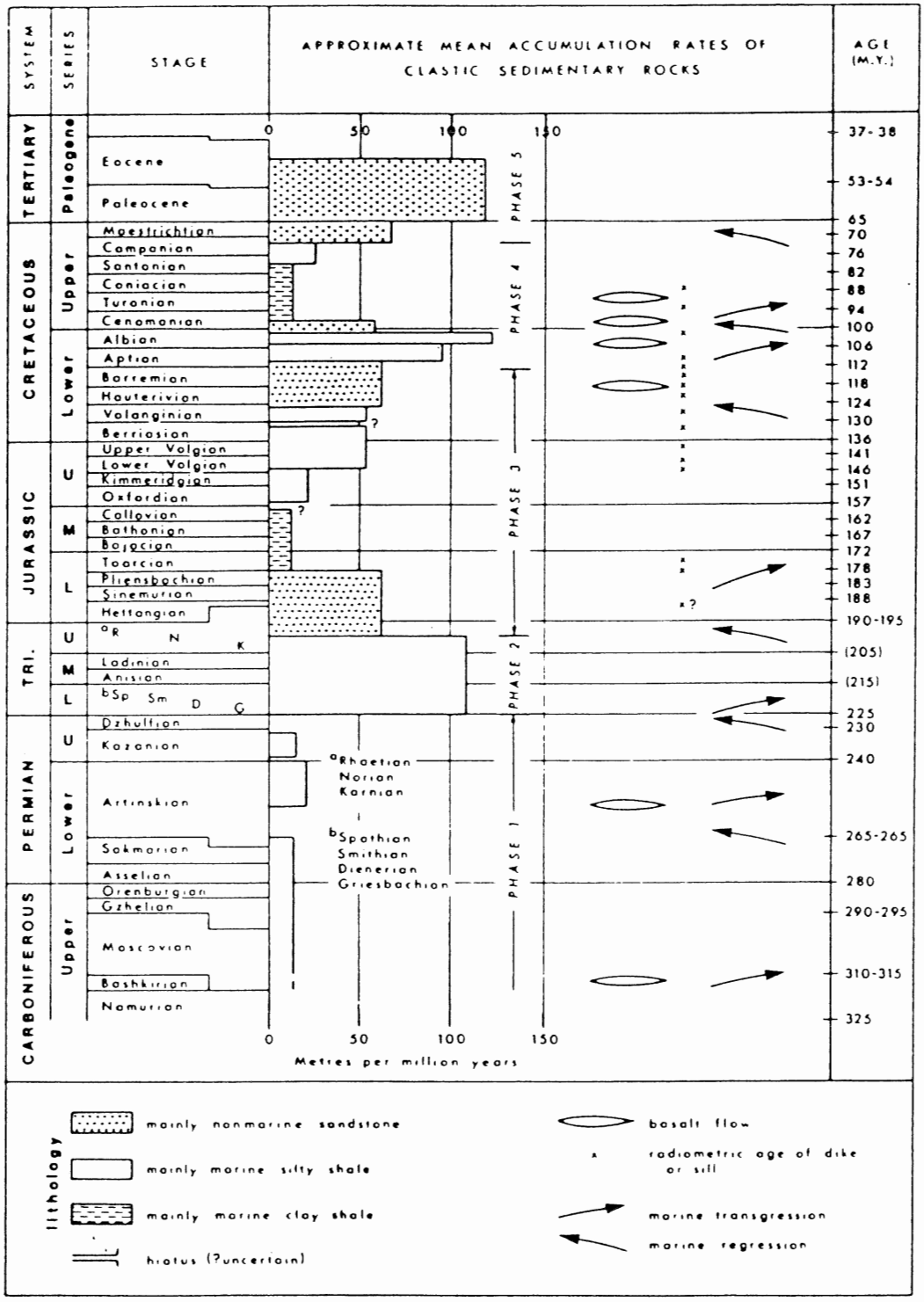

Approximate mean accumulation rates (meters/m.y.) for clastic sedimentary rocks, central Axel Heiberg segment, Sverdrup basin. Thickness data for calculations from Thorsteinsson and Tozer (1970) and Balkwill (in press). Radiometric ages of intrusions from Larochelle et al (1965), Balkwill (in press), and unpublished data furnished by Panarctic Oils Ltd. Data for volcanic episodes from Thorsteinsson and Tozer (1970). Time scale after Douglas (1970).

Figure 2. (After Balkwill, 1978)

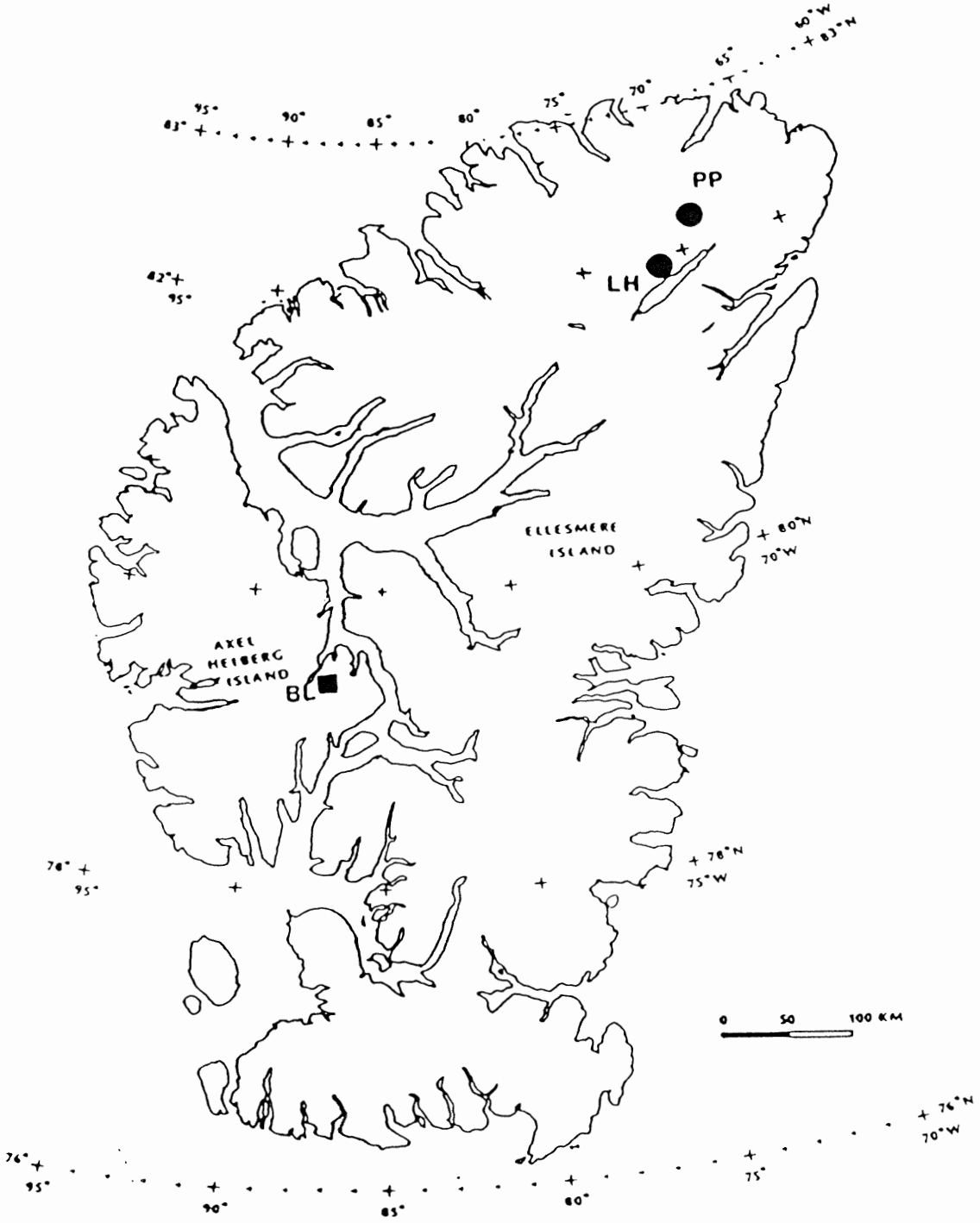

Figure 3. Map of the study area showing sampling sites. Key: PP = Piper Pass; LH = Lake Hazen; BL = Buchanan Lake. (After Williamson, 1985)

The identification of excess argon contained in and diffusive argon loss from crystal lattices has cast doubts upon the reliability of the conventional K-Ar ages obtained. In cases in which excess argon is present, anomalously high ages will be obtained; and in cases in which diffusive argon loss has occurred, anomalously low ages will be obtained. It is very important that accurate ages be known so that models of basin evolution can be derived which will aid in the understanding of the Arctic Ocean (Balkwill,1978); and hence a better understanding of hydrocarbon formation.

A major difficulty in the dating of mafic intrusive and extrusive rocks is the choice of material which will yield the most reliable ages. This is particularly important for mafic rocks because of their low potassium contents. Some workers have suggested that chilled margins will yield the most accurate ages as they cooled rapidly and therefore will yield the exact time of emplacement. Others think that coarse-grained interiors are best, because they are less apt to lose argon through diffusion from grain boundaries than are fine-grained margin samples. Some think mineral separates will give reliable ages because of their relatively simple chemistry, while others feel that although whole rock compositions are more complex, the sum of the argon from all phases will yield an accurate

age where argon redistribution has taken place within a rock (Hanes et al, 1985; Hanes and York, 1978; Bottomley and York, 1976; Lanphere and Dalrymple, 1976; Hanson, 1975; Stukas and Reynolds, 1974).

For this thesis, research has been carried out into the Ar-40/Ar-39 method of dating with the purpose of answering two major questions:

1) Which type of rock component (i.e. fine-grained, coarse-grained, chilled margin, body interior, mineral separate, mafic fraction, felsic fraction, whole rock fraction, altered, or unaltered sample) will yield the most reliable ages for igneous bodies of the type found in the Sverdrup Basin?

2) What are the ages of the four representative igneous bodies sampled for radiometric dating by the Ar-40/Ar-39 method?

The first question was approached by selecting different fractions and samples from single bodies in three locations in the Sverdrup Basin (See figures 1 and 3). These were: 1) a flow overlying the Hassel Formation, which is Albian to Cenomanian in age (Trettin et al,1982; Osadetz et al, in prep.), at Tropical Ridge, Ellesmere Island; 2) Sill #4 from the Star Complex at Piper Pass, Ellesmere Island, which is part of a complex feeder system of dykes and sill represented in figure 4; and 3) a sill and a cross-cutting dyke,

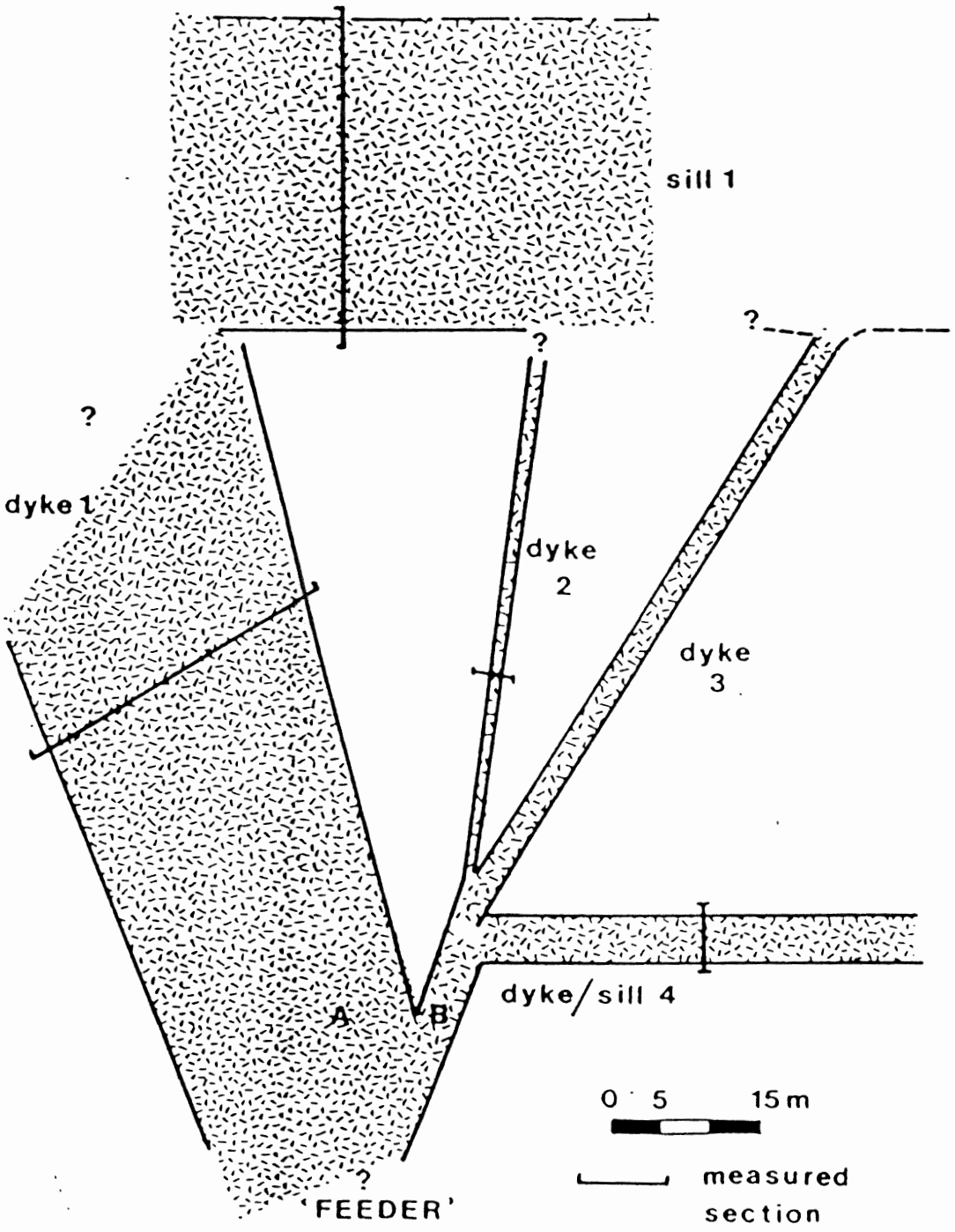

Figure 4. Graphic representation of the geometry of the sills and dykes at Star Complex, Lake Hazen. (After Williamson, 1984)

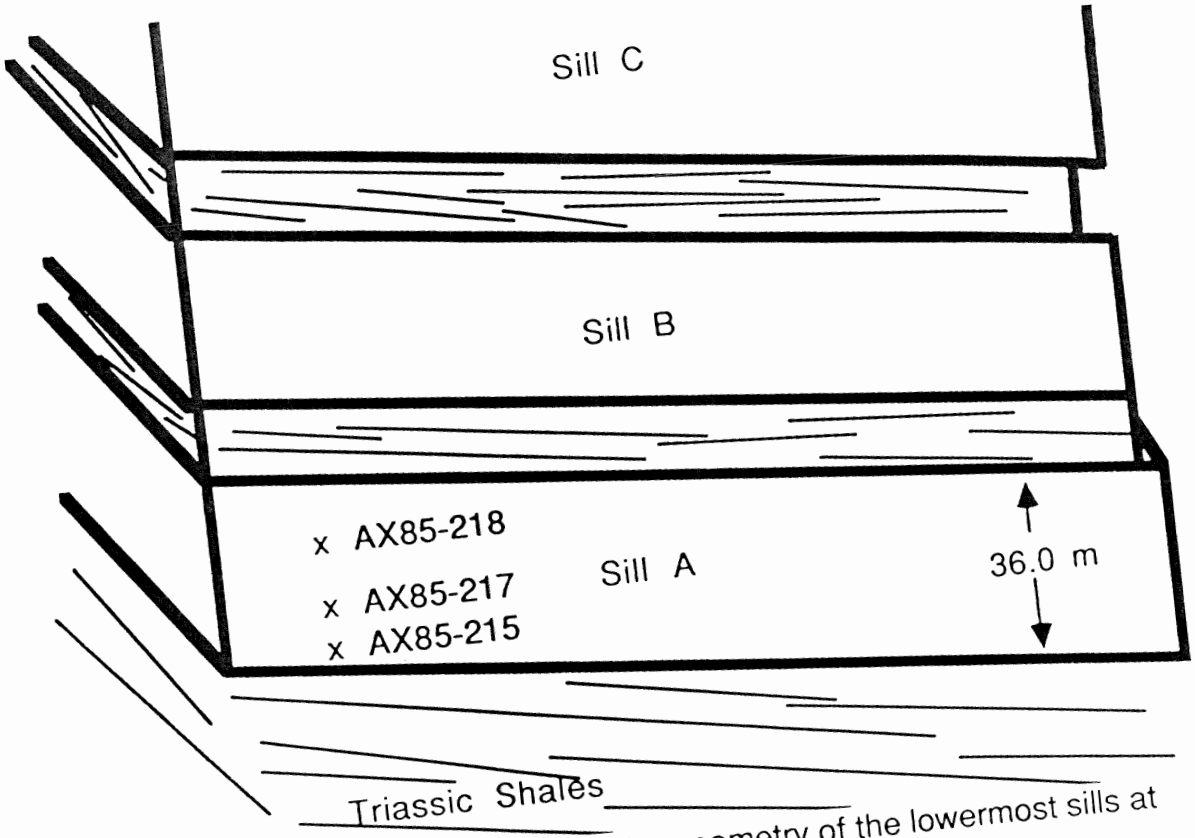

Figure 5. Graphic representation of the geometry of the lowermost sills at Buchanan Lake.

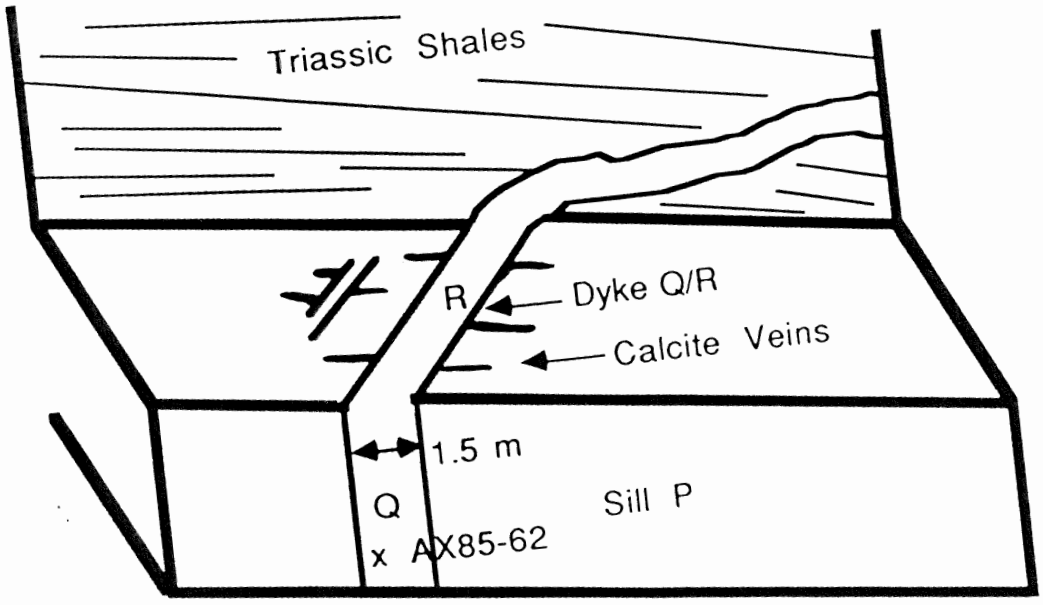

Figure 6. Graphic representation of the uppermost sill (P) and cross-cutting dyke (Q/R) at Buchanan Lake.

intruded near the contact between the Triassic Blind Fjord and Blaa Mountain Formations, Buchanan Lake, Axel Heiberg Island (Figures 5 and 6).

Table 2. Locations of Samples

Location (figure 3)	Sample	Fraction Dated
PP(Tropical Ridge)	EL84-87	Whole Rock
LH(Star Complex)	EL84-49	Whole Rock
	EL84-50	Whole Rock, Felsic
BL(Buchanan Lake)	AX85-62	Whole Rock
	AX85-215	Whole Rock
	AX85-217	Mafic, Felsic
	AX85-218	Felsic, Biotite

By dating more than one sample/fraction from a single body, any differences or disturbances in the age spectra would have to be a function of the sample, and not of the thermal history of the rock. Spectral shapes depend on the chemical composition, mineralogy, and physical geometry of the sample, with particular emphasis on the Ca/K ratios of phases present, and the grainsize of the sample. Also of importance are spectral shapes due in part to reactor induced phenomena such as recoil of argon within a crystal or from one phase to another during irradiation in the reactor.

Once the first question is answered, the best age estimates can be chosen for the bodies sampled, thus resolving the second question.

The purpose of this thesis is to first outline the geological information as it pertains to the chosen samples, and then to outline the Ar-40/Ar-39 method and the mechanisms which produce characteristic spectra. Subsequently, the sample spectra can be analyzed, and conclusions drawn with respect to the questions posed.

Chapter 2. Regional Setting

The complex geology of the Canadian Arctic Islands has been studied since the early 1950's, beginning with the work of Fortier, McNair, Thorsteinsson, and Morley (Fortier et al, 1963). Balkwill (1978) gives a comprehensive account of the regional setting of the Arctic Islands, and the following is a summary of his writing, except where referenced otherwise. (See figure 1).

2.1. Arctic Archipelago

The basement for the Arctic Archipelago consists of granites and metamorphic rocks of the Canadian Shield (K-Ar dated at about 1.7 Ga), overlain subhorizontally by Proterozoic and Phanerozoic sediments. These latter include shallow marine and nonmarine carbonates and clastics, and make up the Arctic Platform. The Franklinian geosyncline of late Proterozoic to early Paleozoic age rests upon the Arctic Platform. It consists of the following:

1) Pearya geanticline, a positive welt which is apparently a source of terrigenous clastic materials for the Hazen trough.

2) Hazen trough, a submarine fordeep trending in a southwesterly direction.

3) a miogeocline formed from the accumulation of carbonate and clastic rocks between the Arctic Platform and the Hazen trough.

During the Ellesmerian orogeny, Middle Devonian to Early Carboniferous, local intrusions and metamorphism, folding and faulting altered the geology of the Franklinian geosyncline. This caused well-developed structural trends to the northeast in northern Ellesmere Island, and to the north in eastern Ellesmere Island.

2.2. Sverdrup Basin

Unconformably overlying the Franklinian rocks is the elongate, northeasterly trending depression called the Sverdrup Basin. It contains marine and non-marine clastic, carbonate, and evaporite strata of Lower Carboniferous to Upper Tertiary age which are up to 13 000 m in thickness. Volcanic extrusives occur as localized packages of flows within the basin sequence. The Sverdrup Basin strata are also cut by abundant diabasic to gabbroic dykes and sills, which have been estimated by various researchers to be from Jurassic to Upper Cretaceous (See table 1 and figure 2).

Based on the geometry and the depositional fabric, Balkwill (1978) suggested that the Sverdrup Basin, now a structural synclinorium, evolved through episodes of crustal fracturing, resulting in periodic subsidence and

Table 1. Previous Radiometric Ages of Igneous Bodies

Location	Body Type	Dating Method	Date	Reference
Blaa Mountain Formation , Ellef Rignes Island	Sill	K-Ar(WR)	118 Ma	Balkwill, 1983 (R.St.J.Lambert, Pers. com.)
Ringnes Formation, Ellef Rignes Island	Sill	K-Ar(WR)	144 Ma	Balkwill, 1983 (R.St.J.Lambert, Pers. com.)
Deer Bay Formation, Ellef Rignes Island	Intrusive sheet	K-Ar(WR)	118 Ma	Balkwill, 1983 (R.St.J.Lambert, Pers. com.)
Ellef Rignes Island	Mafics	K-Ar(WR)	102-110 Ma	Larochelle et al (1965)
N. Grinnell Peninsula Devon Island	Dykes	K-Ar(WR)	114 Ma 112 Ma	Balkwill,l983 (J.W. Kerr, Pers. com., 1976)
NW. Grinnell Peninsula, Devon Island	Basic dyke (chilled margins)	K-Ar(WR)	115±5 117±5	Stevens et al, l982 " "
Amund Central Dome Dome H-40, Amund Ringnes Island	Drill hole	K-Ar(WR)	(l967m depth) 132 Ma (1987m depth) 224 Ma (2464m depth)	Balkwill, 1983 (Panarcticoils Ltd, pers. com.)
Wooton Intrusion, N. Ellesmere Island	Gabbro/Granite Pluton	U/Pb Zircon	92.0±1 Ma	Trettin and Parrish, in prep.
Hanson Point, N. Ellesmere Island	Volcanics	U/Pb Zircon	82+20/-21 Ma	Trettin and Parrish, in prep.
Marvin Peninsula, N. Ellesmere Island	Quartz-diorite Pluton	K-Ar (hornblende)	91.6±9.6 Ma	Stevens et al, 1982
Kleybolte Peninsula, Ellesmere Island	Quartz-bearing Syenite Pluton	K-Ar (hornblende)	73.6±3.5 Ma 84.2±3.9 Ma	Wanless et al, 1977

filling, and also volcanic extrusion and intrusion. Since its formation, the basin has undergone two major episodes of deformation. The Melvillian Disturbance, which occurred between the Late Pennsylvanian and Early Permian, caused localized folding and faulting on the basin margins. Structural deformation has also been noted near the eastern margin. The second disturbance, which caused most of the major structural deformation, especially on Axel Heiberg and Ellesmere Islands, was the Eurekan Orogeny which took place between the Late Cretaceous and middle Tertiary.

Finally, large salt diapirs intruded mainly the southern part of the basin. Nassichuck and Davies (1980) suggested that the salt intrusion was not activated by the Eurekan Orogeny, but rather by normal sediment loading as early as the Jurassic.

2.3. Basaltic Intrusives and Extrusives in the Sverdrup Basin

Basaltic flows, dykes, and sills dated either stratigraphically or isotopically, have been found to be Carboniferous to Upper Cretaceous in age; the oldest are found on northern and central Axel Heiberg Island and the youngest on northern Ellesmere Island (Osadetz et al,in prep; Embry, in prep; Trettin and Parrish, in press). None have been found to cut uppermost Cretaceous or Tertiary strata, and there seems to be a gap in igneous

activity during the Triassic as no radiometric ages have been reported for that period. The latter may be the result of insufficient sampling.

The dykes, generally several meters wide and up to 20 km in length, tend to run parallel with local faults. The sills, up to 100 m thick, commonly span several tens of square kilometers, preferring levels of undercompacted, overpressured shale and siltstone. The phases of igneous activity seem to have occurred during times of accelerated basin subsidence, which caused marine transgression, or during times when sediment accumulation was rapid.

There appear to have been four major episodes of volcanism on Axel Heiberg and Ellesmere Islands during the Cretaceous. The oldest is represented by basalt flows and pyroclastics at the base of the Isachsen Formation, which is of Valaginian to Aptian age (Osadetz et al, in prep; Embry, in prep). These flows outcrop at Geodetic Hills and Bunde Fjord, Axel Heiberg Island. The second episode consists of a minor amount of extrusives found within the Walker Island Member of the Isachsen Formation (Osadetz et al, in prep.; Embry, in prep.). These flows, which outcrop at Camp Five Creek, near Bunde Fjord, were extruded during the late Barremian to early Aptian. The third episode is represented by the Strand Fjord Formation,

extruded in the interior of the Sverdrup Basin. During this episode, a major amount of extrusion took place. Over 800 meters of flows, localized mainly on western Axel Heiberg Island, outcrop at Bunde Fjord, Bals Fjord, and Strand Fjord (Osadetz et al, in prep.; Embry, in prep.). Although provisionally assigned to the Late Cretaceous by Osadetz et al (in prep.), the Strand Fjord Formation has since been dated paleontologically to be of late Albian age (Embry, A., verbal com.), thus separating it from the fourth and youngest volcanic episode. Volcanic flows and pyroclastics of the fourth episode can be found within several Late Cretaceous formations, including those at Emma Fjord, Phillips Inlet, and Hanson Point (Osadetz et al, in prep.;Trettin, in press). Evidence to date indicates that these youngest volcanics were extruded primarily at the basin margin.

In addition to radiometric ages and stratigraphic relationships, paleomagnetic information has the potential to aid in distinguishing between flows from different episodes. Rapid polarity changes in the Neocomian, each spanning less than two million years, can provide a check on the ages obtained by isotope dating, especially if the rocks dated are reversely polarized. The third and fourth Cretaceous volcanic episodes occurred during the 'quiet period' of the Cretaceous, when the Earth's

polarity remained normal for over 30 Ma. Conversely, the first and second episodes took place during the Neocomian, and therefore there is the possibility that volcanics of the earlier and later episodes may be distinguished on the basis of paleomagnetism (Jackson and Halls, 1983). This information could aid in checking the accuracy of the radiometric and stratigraphic ages obtained.

Chapter 3. Method of Ar-40/Ar-39 Dating

3.1. Introduction

It is well understood that radioactive isotopes decay over time to stable isotopes by processes such as electron capture, ß-particle emission, or ∝-particle emission. The decay lifetime, measured in half-lives, may be a fraction of a second to billions of years or more. When the half-life of a particular isotope found in rocks is of the same order as the age of the rocks, that decay relationship may be used to date the time of formation or cooling. The dates are found by measuring the ratios of the parent (radioactive) and daughter (stable) isotopes. For example, K-40 is radioactive and it decays to Ar-40 through electron capture, with a half-life of 1.3 billion years. In the conventional K-Ar dating method, the K-40 concentration is measured separately, usually by flame photometry, and the Ar-40 concentration is measured by mass spectrometry. Errors associated with these two different methods introduce uncertainty into the dates obtained.

For the above reason, a means of determining the parent/daughter ratio by one and the same method was explored (Turner, 1969). Relative abundances of K-40 and K-39 (i.e. [K-40] = [K-39] / 7.99×10^3) are assumed

to be approximately constant over time. By bombarding the K-39 with fast neutrons in a nuclear reactor, one can produce Ar-39 via the reaction K-39(n,p)Ar-39 and this isotope can be measured by a mass spectrometer along with the Ar-40 measured in the conventional K-Ar method. One can obtain an age using the equation:

$$t = 1/\lambda \ln \{ 1 + J (Ar\text{-}40^*/Ar\text{-}39) \} \quad (1)$$

where t is the age of cooling, λ is the total decay constant of K-40 which decays by a branching scheme to Ca-40 as well as Ar-40, Ar-40* is the concentration of radiogenic Ar-40, and J is an irradiation parameter, dependent upon the neutron flux at the location of the sample in the irradiation canister. To find J, a standard of known age must be irradiated along with the sample of interest. For the analyses reported in this thesis, standard MMhb-1, a hornblende from McClure Mountain, Colorado, was used. Corrections are made for differing positions in the canister, and for atmospheric argon, as well as for interfering isotopes (Dallmeyer, 1979).

After irradiation, the sample may be fused in one step, the Ar-40/Ar-39 ratio measured by mass spectrometry, and the age calculated by equation (1), giving an age which should be analagous to the conventional K-Ar age (Dallmeyer,1979). Because the Ar-40/Ar-39 method deals only

with ratios and not with absolute quantities in the rock, the sample does not have to be outgassed all at once. It can be heated up in steps and each step analyzed individually, yielding an apparent age corresponding to each temperature. The apparent ages are plotted as a function of temperature (or cumulative % Ar-39) to produce an age spectrum. Plots of this type can give an indication of the reliability of the ages obtained. This technique allows a measurement of ages from argon ratios, supposedly representing different sites or phases of minerals and rocks (Hanson,1975).

3.2. J-Values

J-values are obtained from the analyses of standards (i.e. mineral separates which have been dated by many techniques and whose ages are internationally accepted), placed at intervals throughout the irradiation canisters.

In equation (1),

$$J = 7.99 \times 10^{3} \lambda/\lambda_{\varepsilon} \Delta T \int \phi(\varepsilon) d\varepsilon \qquad (2)$$

where λ_{ε} is the decay constant for electron capture by K-40, ΔT is the irradiation time, and $\phi(\varepsilon)$ is the neutron flux of neutrons with energy ε (Elias, 1986, unpub. Ph.D. thesis). When t is known, J becomes:

$$J_s = \left[\frac{\text{Ar-39}}{\text{Ar-40}}\right]_s e^{\lambda t_s} - 1 \quad (3)$$

Values of J for individual unknown samples may be determined by interpolation of known values (See figure 7). Once J is known for a sample, t is easily calculated, assuming the Ar-40/Ar-39 ratio has been determined.

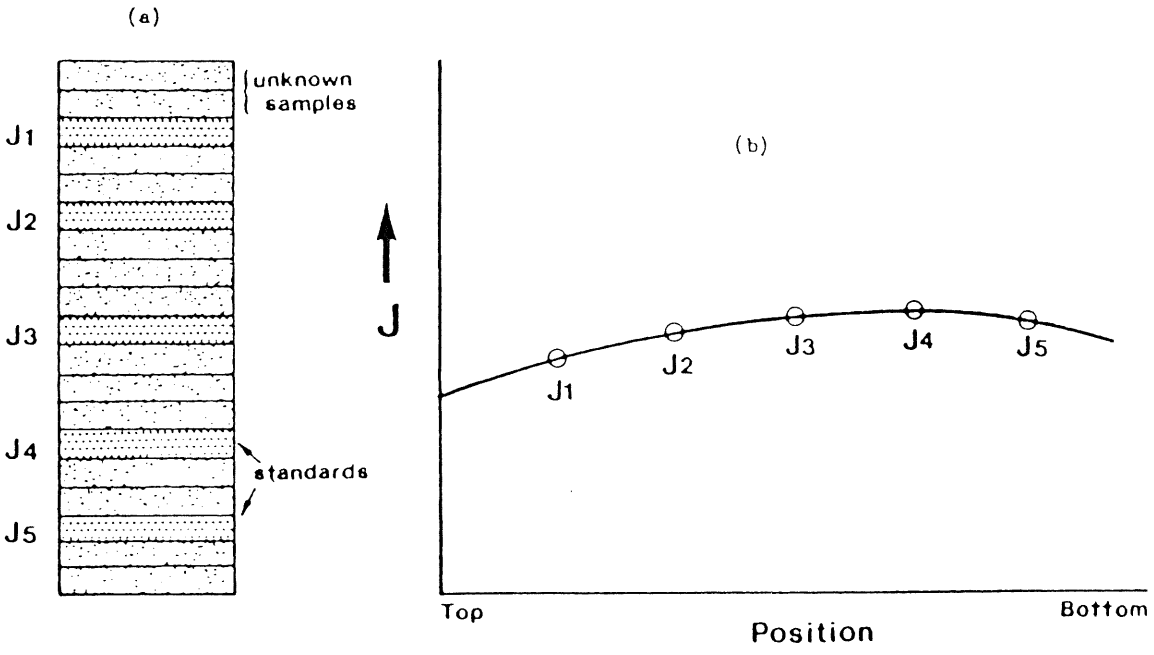

Figure 7. Showing a) placement of standards in irradiation canisters and b)determination of sample J values by interpolation. (After Elias, unpub., 1986)

3.3. Interfering Isotopes

In the nuclear reactor K-39 is irradiated to produce Ar-39, but this is not the only reaction which takes place. In addition, argon isotopes from

Table 3.

Isotopes generated during neutron irradiation of K-bearing phases in a reactor (Brereton, 1970).

Argon Isotope Produced	Ca Reaction	K-Reaction
36	$^{40}Ca(n,n\alpha)$	
37	$^{40}Ca(n,\alpha)$	$^{39}K(n,nd)^{+}$
38	$^{42}Ca(n,n\alpha)$	$^{39}K(n,d)$; $^{41}K(n,\alpha)$
39	$^{42}Ca(n,\alpha)$; $^{43}Ca(n,n\alpha)$	$^{39}K(n,p)$; $^{40}K(n,d)$
40	$^{43}Ca(n,\alpha)^{+}$; $^{44}Ca(n,n\alpha)^{+}$	$^{40}K(n,p)$; $^{41}K(n,d)$

+ Negligible quantities

mass 36 to mass 40 are produced from Ca and K isotopes in the sample.(See Table 3). Because the Ar-38 concentration is irrelevant to the age calculation, it can be ignored, as can Ca- derived Ar-40 and K-derived Ar-37, which are produced in negligible quantities. Before final age calculations are carried out, corrections must be made for K-derived Ar-40, and Ca-derived Ar-39 and Ar-36. The concentration of Ar-37, produced almost exclusively from Ca, and the concentration of K-derived Ar-39, are proportional to the Ca/K ratio in each outgassing step, which is often characteristic of a particular mineral.

3.4. Sample Preparation

In total, age determinations were carried out on ten fractions from seven samples in three locations. These consisted of five whole rock sampless, four felsic or mafic fractions, and one mineral separate.

The seven samples were crushed using a tungsten-carbide shatterbox, and then sieved and washed to obtain the 80 to 120 mesh size fraction. Mineral separation was carried out by first removing the highly magnetic fraction using a Franz magnetic separator, and then by tuning the Franz to obtain progressively cleaner mineral fractions. This method was used to obtain good quality fractions of biotite, mafics, and felsics. Finally, these samples were hand-picked using an optical microscope, to obtain a high degree of purity (99%). Where biotite was present in the rock (AX85-217,AX85-218), it was extremely important that the biotite was completely removed from the felsic and/or mafic fractions as it has a much higher potassium concentration than any of the other phases . Otherwise, the argon signals obtained from the biotite contaminant would have overwhelmed the argon signals derived from the mineral(s) of interest.

Aliquots of approximately 200 mg of the whole rock samples or mineral separates and standards were wrapped in aluminum foil and then

placed into aluminum canisters lined with cadmium, a thermal neutron absorber. The canisters were then sent to the McMaster University nuclear reactor and irradiated for approximately 10 hours. Cooling periods of between one and three months were allowed so that isotopes with relatively short half-lives would decay before the samples were handled in the laboratory.

3.5. Ar-40/Ar-39 Dating Procedure

Samples were placed in a quartz boat and then set in a quartz furnace which has the capability of heating to 1200°C. The temperature is thermostatically controlled by a thermocouple placed directly beneath the quartz furnace. The furnace is attached to a glass line which contains a titanium getter which absorbs volatile gases, a charcoal finger for argon adsorption, and a cold trap which aids in the removal of any residual gases prior to admission of the sample to the mass spectrometer. (See figure 8).

A typical step in the dating procedure consisted of 1) increasing the furnace temperature by 50°C and allowing the sample to outgas for one hour, 2) lowering the charcoal temperature to -196°C by immersing in liquid nitrogen, thus adsorbing argon and other gases onto the charcoal, 3) a) closing off the extraction furnace and b) isolating the sample, 4) heating the

titanium to 800°C for 10 minutes while pumping out the line in order to purge the titanium of residual gases bound to the it during the previous step, thus producing a fresh titanium surface, 5)allowing the sample gas to interact with the titanium for twenty minutes during which time volatile gases bonded to the titanium, leaving relatively pure argon, 6)freezing the sample over into the sample inlet section, and 7) admitting the sample to the mass spectrometer for argon isotope measurement.

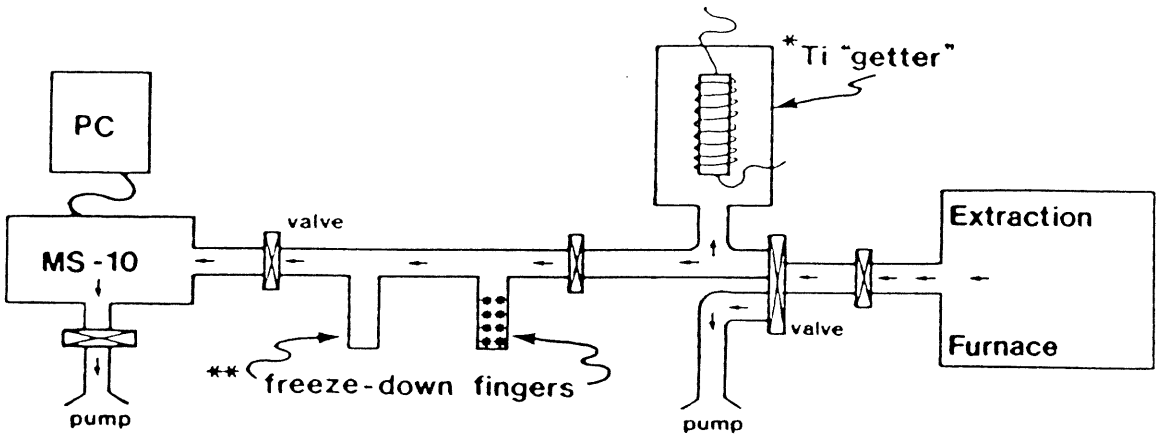

Figure 8. Schematic diagram of argon gas extraction system. (After Grist, unpub., 1986)

3.6. Mass Spectrometer

The mass spectrometer used is a modified AEI-MS-10 which operates on analog signals. The ion source is a rhenium filament. The source supply voltage is modulated by a Apple IIE computer which operates on digital signals. Modifications to the original AEI-MS-10 include an ion current

amplifier and an accelerating voltage amplifier. A Dana Industries digital voltmeter digitizes the accelerating voltages from the peaks so that the signals can be understood by the computer. The Apple IIE incorporates a digital to analog converter so that operating signals can be sent back to the AEI-MS-10.

For each temperature step in the outgassing procedure, 15 measurements were made of the Ar-36, Ar-37, Ar-39, and Ar-40 peaks; and the ratios of Ar-36/Ar-39, Ar-37/Ar-39, and Ar-40/Ar-39 calculated. The Ar-36/Ar-39 and the Ar-40/Ar-39 trends were extrapolated to zero time, for use in the age calculation.

3.7. Representation of Data

Data obtained by the Ar-40/Ar-39 method are represented in two ways. The first is a graph of incremental ages plotted as a function of experimental temperature (often expressed as cumulative percent Ar-39 released), giving an "age spectrum" for the sample (Dallmeyer,1979). A discussion of the implications of different types of age spectra, including possible thermal histories, will follow later. The second method is referred to as an "isochron diagram". The points are obtained from the incremental gas fractions of the step heating analysis, rather than from several

different samples with similar geologic settings as is necessary to create a K-Ar isochron plot (Dallmeyer,1979). In an isochron diagram, the Ar-40/Ar-36 ratio is plotted against the Ar-39/Ar-36 ratio, yielding a line with a slope equal to the Ar-40/Ar-39 ratio, which may be used to calculate an age, t, according to equation (1), and an intercept equal to the Ar-40/Ar-36 ratio, which is assumed to be the original argon ratio (Merrihue and Turner,1966) (See figure 9). These plots can yield information which is not apparent through studying the age spectra, and vice versa.

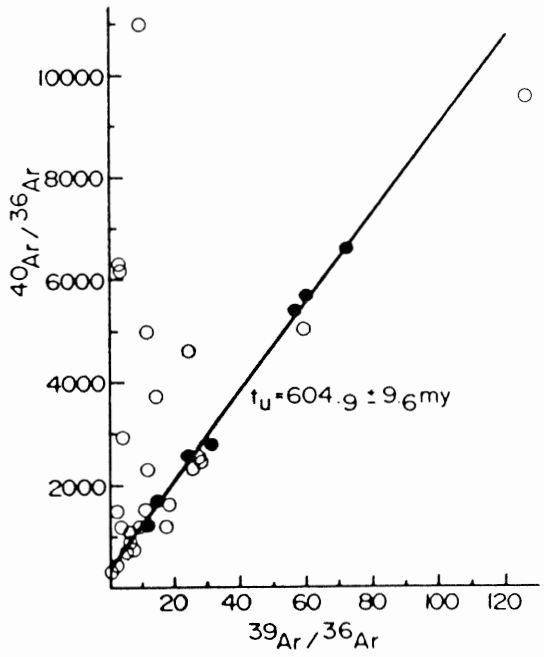

Figure 9. An isochron plot of Long Range Dyke, Newfoundland data. (After Stukas and Reynolds, 1974, p. 263)

Chapter 4. Theory Behind Spectral Interpretation

4.1. Ideally Simple Thermal Histories -- Plateaux Spectra

The simplest form of spectrum is derived from a sample which has effectively cooled geologically instantaneously (York,1984). An example of rocks from this category are the Texas tektites which were formed in short-lived, high temperature events and subsequently remained undisturbed (York,1984). If a sample does not contain any extraneous argon, and if it has neither gained nor lost any potassium or argon (except for the accumulation of radiogenic Ar-40 from the decay of K-40), the Ar-40/Ar-39 concentration ratio should be the same for each temperature step, yielding a plateau age; and this plateau age should be equal to the total gas age defined by the argon ratio of the sum of all of the steps. The spectrum is then said to be concordant (See figure 10).

Concordant spectra can also be produced when a sample is thermally disturbed to such a degree that its original spectrum is completely overprinted (refer to section 4.2). The plateau age in such a case then represents the time of the thermal disturbance. Complete overprinting usually requires temperatures above 600°C (York,1984; Dallmeyer, 1979).

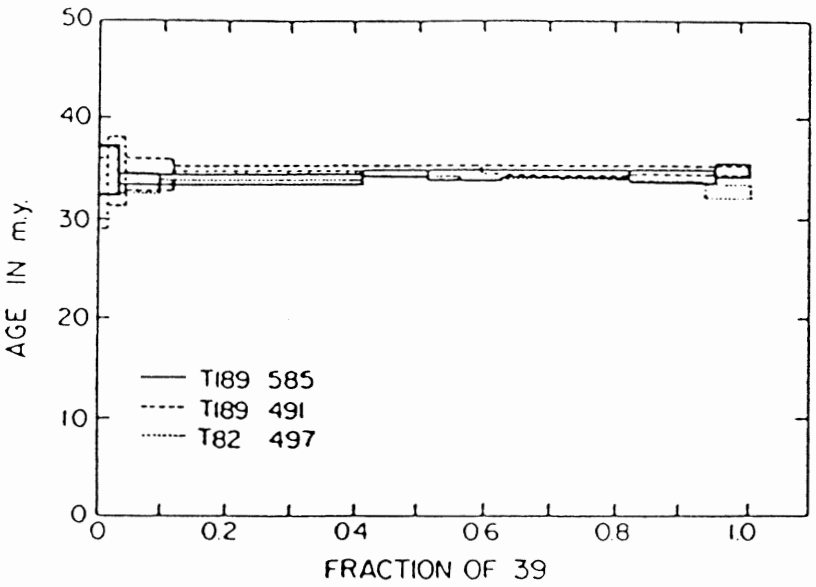

Figure 10. Three Texas tektites showing plateau spectra.(After York, 1984, p. 385)

4.2. Single Pulse Thermal Histories -- Disturbed Spectra

In theory, the simplest deviation from the ideal is derived from a sample which has cooled instantaneously, but later experienced a brief thermal disturbance in an otherwise undisturbed history (York,1984). The first interpretation of these spectra was made by Turner et al (1966), who assumed that radiogenic argon loss during the thermal pulse was governed by simple volume diffusion from spheres. He noted that the lowest temperature fraction in the spectrum will give a maximum to the time of occurrence of the pulse. In addition, it was noted that the smaller the gas fraction extracted in the first step, the closer would be the minimum age to

the actual age of the pulse. These spectra usually showed an increase in apparent age from the low temperature fraction to the high temperature fraction with the observed shape of the spectra being a function of the extent of diffusive argon loss as well as the geometry of the sample

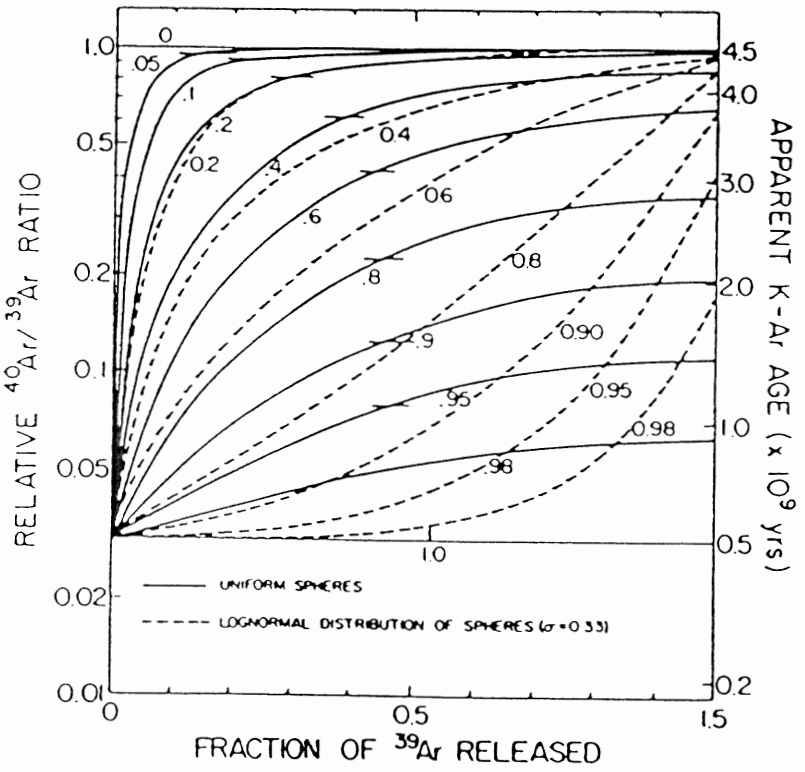

Figure 11. Model age spectra for samples of initial age 4.5 Ga that have suffered, to differing degrees, a degassing event 500 Ma ago. The numbers on the curves indicate the different fractions of argon lost in the event. (York, 1984, p. 386; After Turner, 1969)

(Turner,1969) (See figure 11). Ideally, a thermally overprinted spectrum could yield the time of reheating (at the low temperature end of the

spectrum), as well as the time of initial argon retention (at the high temperature end), although sometimes the sample is overprinted to such an extent that the original retention age is completely obliterated from the record (Dallmeyer,1979). Hanes and York (1978) noticed this phenomenon in an Abitibi dike from the Canadian Superior Province. In that case, the age of an Hudsonian hydrothermal event was found from a partially overprinted sample. Also, Ozima, Kaneoka, and Yanagisawa (1978) found in their laboratory experiments on the effects of temperature and pressure on Ar-40/Ar-39 systematics that partial argon loss resulted to varying degrees, and was reflected in their results, producing spectra very similar to those of geologically disturbed samples.

4.3. Very Slow Orogenic Cooling -- Blocking Temperatures

A third type of thermal history is the case of very slow postorogenic cooling. Turner (1969) made a point in his paper that if a mineral were cooling slowly after formation, and not disturbed afterwards, the argon concentration profile would be "superficially similar" to that produced by an episodic loss of argon (See figure 12). By using a combination of estimated temperatures and corresponding times for slow cooling terrestrial materials, it is possible to calculate simultaneously both the time when a

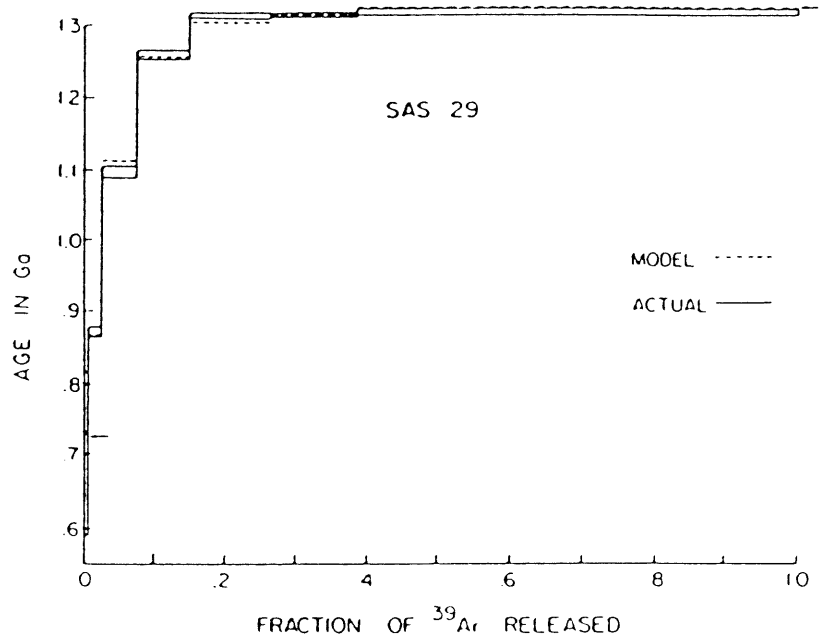

Figure 12. Experimentally determined age spectrum of an illite (York et al, 1981). The best-fitting least-squares matching spectrum was derived by Hall and York (1982). (After York, 1984, p. 390)

mineral became a closed system for argon diffusion and also the temperature at which that closure occurred, known as the "blocking temperature" (York,1984) (See figure 13). By dating different minerals from the same slowly cooled rock body and obtaining a series of ages and corresponding temperatures, one can obtain a cooling curve i.e. a temperature vs. time plot (York,1984). This is possible because different minerals are characterized by different blocking temperatures as

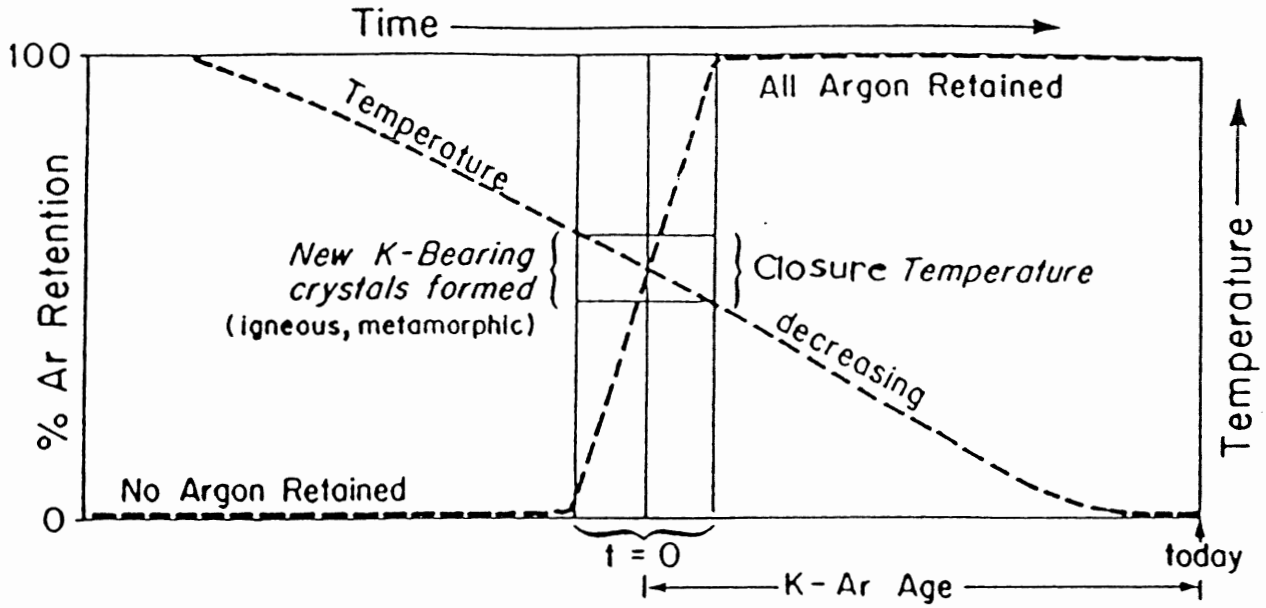

Argon Accumulation in K-Bearing Mineral with Simple History

Figure 13. (After Elias, unpub., 1986)

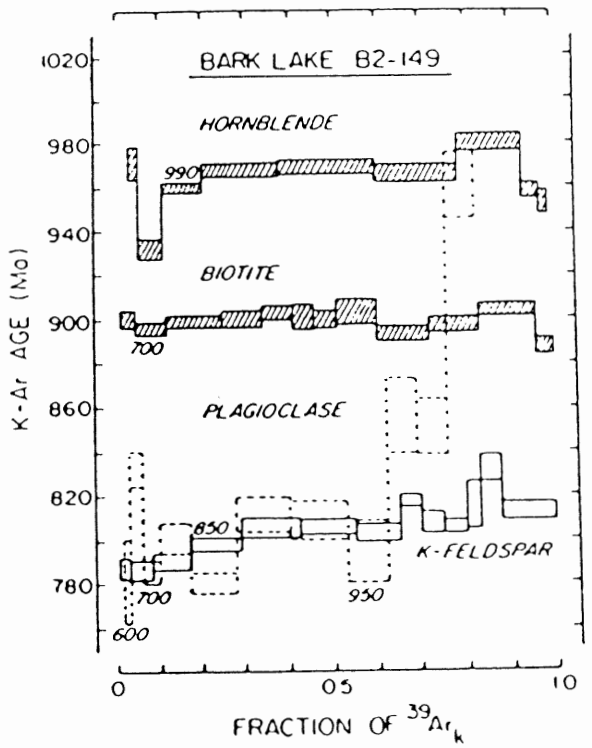

Figure 14. Age spectra from a single diorite hand sample (Berger and York, 1981a). (After York, 1984, p. 395)

illustrated in figure 14. Note that the four mineral separates from the same hand specimen yield four different ages.

4.4. Effects of Excess Argon on Ar-40/Ar-39 Dating

Following usage in Lanphere and Dalrymple (1971), "excess argon" is defined in this paper as Ar-40 incorporated into rocks and minerals by processes other than internal decay of K-40 to Ar-40. "Inherited argon" originates within the minerals by internal decay of K-40 prior to the rock forming event. The term "extraneous argon" includes both excess and inherited argon.

The possibility of excess argon was noted by Lanphere and Dalrymple (1976) in their studies of Liberian diabase dykes. They describe two samples of known age (Jurassic), which gave anomalously old K-Ar ages. The Ar-40/Ar-39 age spectra of these samples are "saddle-shaped" (i.e. the apparent age of successive gas fractions decreases to a broad minimum at intermediate temperatures, and then increases until all of the argon is released) (See figure 15). It was also shown that isochron plots of the Ar-40/Ar-39 data did not reveal the crystallization ages of the rocks. Stukas and Reynolds (1974), in their studies of the Long Range dikes in

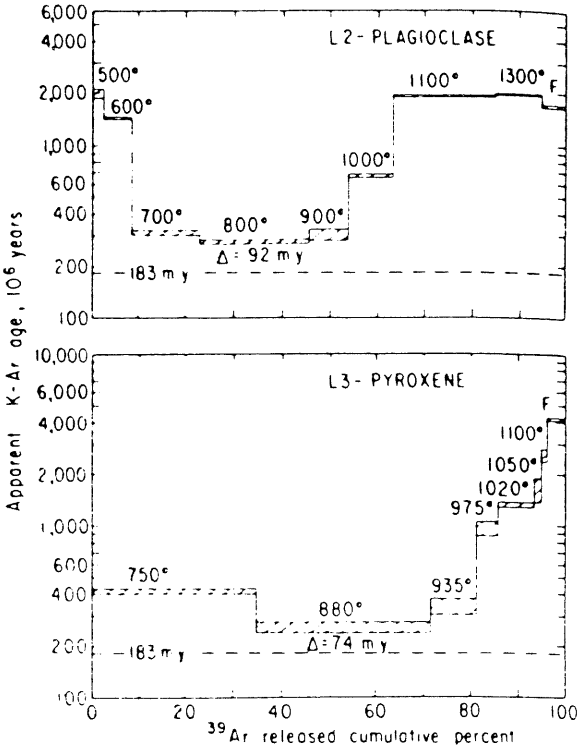

Figure 15. Ar-40/Ar-39 spectra from minerals known to contain excess radiogenic Ar-40. The dashed lines indicate the approximate age of crystallization. (After Lanphere and Dalrymple, 1976, p. 144)

Newfoundland, found anomalously high apparent ages in the high temperature fractions for most of their samples. This they attributed to excess radiogenic argon. Saddle minima are usually found to be only an indication of the maximum possible age of the samples (Lanphere and Dalrymple,1976). Lanphere and Dalrymple (1976) suggest that there are no independent criteria which can distinguish a geologically meaningful age from a

maximum possible age in saddle-shaped spectra. Conversely, they suggest that the scatter of data on the isochron plot can be used as an unambiguous indicator that a particular sample does not fulfill the assumptions of the K-Ar system. An hypothesis which sufficiently explains the reason for a saddle-shaped spectrum has not yet been proposed.

4.5. Effects of Loosely Bound or Redistributed Argon on Ar-40/Ar-39 Dating

The loss of loosely bound argon, or the redistribution of the argon retained within a rock can cause complex age spectra which are often difficult to interpret. The difficulty arises because the minerals in the rocks are interrelated in ways which are so complex that they are not understood at present, and therefore particular behaviour is difficult to predict.

For example, Leech (1966) noted in his study of basic intrusive rocks in the N.W.T., that chilled margins tend to yield older K-Ar ages than central samples. He argued that this was due to abundant biotite found at the chilled borders which preserved the primary whole rock ages, while central samples with abundant feldspar alteration suffered argon loss. Leech (1966) did suggest, though, that where the feldspars were deuterically

altered to sericite primary whole rock ages were retained within coarse-grained central samples. Hanes and York (1978) found that the interiors of the Abitibi dykes from the Canadian Superior Province are more retentive than the margins. Through microprobe analyses they found that sericite, found only in the samples from the interior of the dyke, was the high potassium phase relative to all other phases within the rock and therefore it was reasonable to think that the potassium was redistributed through the rock during alteration, thus yielding a "staircase" type of spectrum (See figure 16). York (1984) refers to the age spectra of

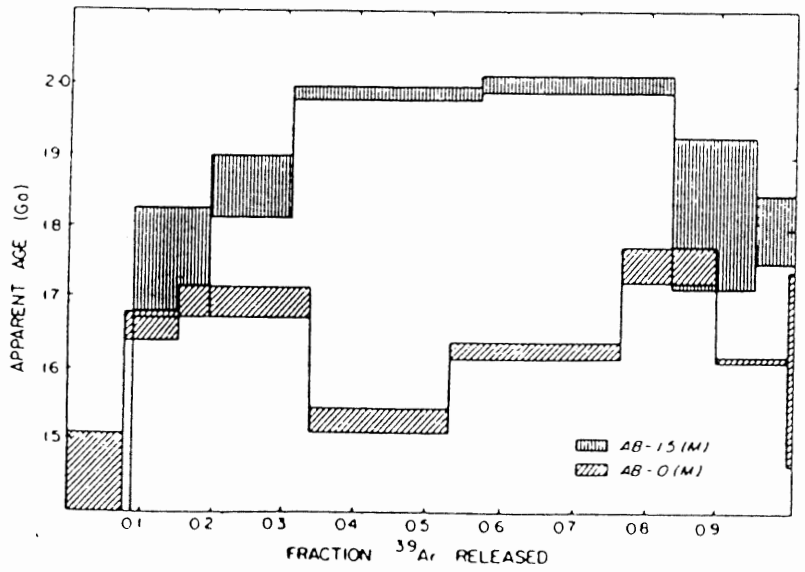

Figure 16. Staircase-shaped spectrum from the Abitibi Dyke, Canadian Superior Province. (After Hanes and York, 1978)

chondrites which exhibit erroneously high ages in the low-temperature portion of the spectrum, perhaps due to argon redistribution during partial melting.

Hanson (1975) evaluated the Ar-40/Ar-39 method for dating Precambrian mafic rocks. He submitted that if a rock has undergone partial loss of radiogenic argon, and if the sites that lose radiogenic argon readily in nature also lose argon more readily in a vacuum furnace, then higher temperature fractions will give progressively higher ages. If there is little argon loss, or if the sites which lose argon in nature lose all of their argon at low temperatures in the vacuum furnace, then a plateau spectrum will be observed at higher temperatures.

Stukas and Reynolds (1974), in their study of eleven samples from the Long Range dykes in Newfoundland, found extremely wide age variations in both the low and the high temperature regions. The medium-temperature region of the age spectra is characterized by a relatively narrow range of apparent ages for all but one sample (See figure 17). The medium-temperature fractions, when taken as a group and plotted on an isochron diagram, were much more highly correlated than either of the other regions. It was suggested that in this temperature interval the outgassing of

unaltered plagioclase was being observed, but no explanation was submitted for the complexity in the rest of the spectrum.

Sometimes very complicated spectra can be integrated to give ages that are in agreement with K-Ar, Sr-Rb, or U-Pb dates (Bottomley and York,1976; Hanes and York,1978). This indicates that a closed-system redistribution of argon has likely taken place in the samples (Bottomley and York,1976). In cases such as this, the most disturbed sample tends to yield both the highest low-temperature age and the lowest high-temperature age, or vice versa, which is in keeping with the redistribution model. The mechanism for such a closed system redistribution is not yet clear (Bottomley and York,1976) as is the case for all but the simplest scenarios.

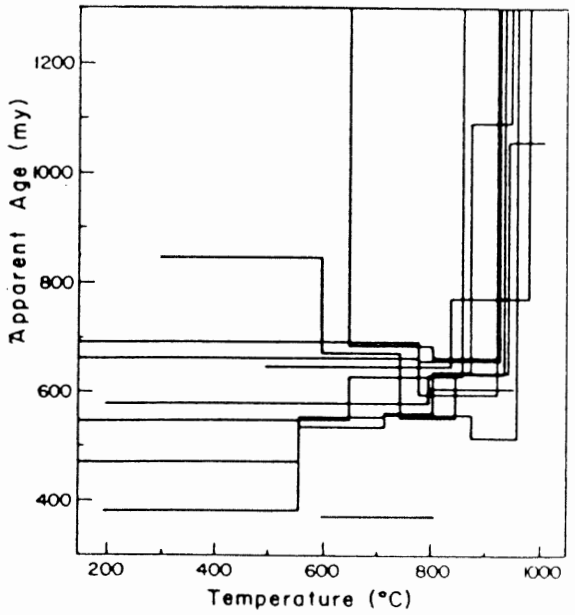

Figure 17. Ar-40/Ar-39 Age spectrum plot showing data for all the Long Range Dyke samples. (After Stukas and Reynolds, 1974)

Chapter 5. Sample Descriptions

Seven samples, collected by Marie-Claude Williamson and Dr. Gunter K. Muecke from the Department of Geology, Dalhousie University, were selected for radiometric dating using the Ar-40/Ar-39 technique. Each of these samples was from an intrusive or extrusive unit for which an age could only be speculated upon, as stratigraphic relationships which would indicate a precise age were not present.

The samples were taken from three locations (sample mineral compositions are summarized in table 4):

1)Tropical Ridge, near Lake Hazen, northern Ellesmere Island (location LH, figure 3). Its fine-grained (<1mm) hypocrystalline texture and the fact that there are no overlying sediments suggest that it is a flow. This sample (EL84-87) contains 5-10% moderately altered glass, and its plagioclase is somewhat altered to sericite and sausserite. The sample was taken 21.0 meters from the base of a 21.5 meter section which displays two cooling units. It is dark grey, very finely crystalline, massive, and shows no apparent alteration. According to Williamson's 1984 field notes, minute rounded olivine phenocrysts (1-2%) were present in this portion of the unit, which also shows columnar development. Minute calcite and glass-filled

Table 4-Sample Mineralogy

M=Mafic Separate F=Felsic Separate z=Zoned a=Altered Glass	Samples						
	EL 84-87	EL 84-49	EL 84-50	AX 85-62	AX 85-215	AX 85-217	AX 85-218
Grainsize:							
matrix	<1mm	<0.4mm	<0.5mm	<0.3mm	<0.5mm	0.4to1 mm	1to4mm
phenocrysts	---	up to 3mm	up to 2mm	up to 1mm	up to 2mm	up to 3mm	up to 1cm
Degree of alteration	moderate	high	slight	slight to moderate	high	moderate	moderate
glass	a5-10%	a20%	10-15%	a5%			
K-feldspar							5% F
quartz						10%	5% F
plagioclase	35%	z 30%	z 25%F	z 30%	25%	z 20% F	z 20% F
muscovite/sercite	<3%	10%			10%	10%	10%
iddingsite/chlorophaeite				5-10%			
chlorite					<10%	7%	10%
apatite			<3% F		<3%	5%F	<5% F
biotite					10%	<5%	5%
hornblende			<5%		<5%	8% M	<10%
clinopyroxene	30%		30%	35%	15%	25% M	20%
carbonate (calcite)		~20%	<5%		<5%	<5%	
oxides (opaque mins)	15%	20%	15%	20%	20%	10%	10%
olivine	10%		5%	<5%			

vesicles were noted, and can be observed in thin-section. Despite the presence of amygdales, no conclusive evidence was available which would indicate that this unit was extruded.

2) Star Intrusive, Star Complex (location PP, figure 3). This complex intrudes the Trold Fjord formation which is Late Permian in age (Mayr et al, 1982a). Two samples were selected for Ar-40/Ar-39 dating from Sill #4, which has a total thickness of 10 meters (See figure 4). The first is a sample of the chilled margin (EL84-49), within 8 cm of the contact with sediments. This sample is glomerophyric and hypocrystalline, with phenocrysts up to 3mm and matrix up to 0.4 mm. It is highly altered showing plagioclase altering to sericite, and devitrified glass (5-10%). The handsample is light grey, finely crystalline, and massive, and shows 1-2% sulphides as well as common plagioclase phenocrysts up to 3mm in size. Williamson noted that within a few centimeters of this sample, the rock rapidly turns to a dark green, with more mafics, and becomes considerably coarser.

The second sample (EL84-50) was obtained 2.5 m above the base of the sill. This is a pristine sample which is glomerophyric and hypocrystalline. The phenocrysts range up to 2 mm, while the matrix is generally <0.5 mm.

generally <0.5 mm. The glass (5-10% of the rock) is both fresh and devtrified, and the plagioclase is only slightly altered. In hand sample, this is a darker grey than the first sample, and has a massive, medium-grained, sugary texture. Some of the pyroxene grains are up to 2 mm in size.

The Star Complex is expected to be approximately Cretaceous in age as it seems to be related petrologically and geochemically to volcanic rocks overlying the Hassel formation at Tropical Ridge and Arctic Hare mesa. These are exposed 50 km from this locality (Osadetz et al, in prep.; Williamson, pers. com.).

3) Buchanan Lake Sills (location BL,figure 3).

Sill A (36m thickness): Three samples were selected from this, the lowest of sixteen sills in the section (See figure 5). Sill A contacts sharply and conformably with hornfelsed, fissile, black siltstones and shales, and its base is exposed in places (Muecke, 1985 field notes). At the contact, the diabase is extremely fine-grained with abundant sulphide blebs 1 to 2 mm in size.

The first sample, AX85-215, was taken 30 cm above the base of the sill. This sample is holocrystalline and glomerophyric, with phenocrysts up to 2mm and matrix generally <0.5 mm. The major K-bearing phases are

primary biotite (15%) and sericite alteration of feldspar (<10%). It is medium-grey with brownish-grey weathering products and is very fine-grained. Plagioclase phenocrysts (1 to 2 mm) and sulphide blebs (up to 1 mm) are scattered throughout the rock.

The second sample, AX85-217, taken approximately 13 m above the base of the sill, is holocrystalline granular, showing intergranular textures. Its grainsize ranges from 0.4 to 1.0 mm, with minor phenocrysts up to 3mm. This sample is moderately altered. The hand sample is medium-grey diabase with darker grey weathering. Phenocrysts of pyroxene and plagioclase (up to 3 mm) and minor sulphides are present.

The third sample, AX85-218, taken 24.0 m above the base of the sill, is holocrystalline and phaneritic having many grains up to 4 mm or more. This sample is also moderately altered, the K-feldspar (<5%) and the plagioclase altering to sericite. Biotite (<5%) is also present. The hand sample is medium-grey with darker brownish-grey weathering products. It is a coarse-grained to pegmatitic diabase which has pyroxene crystals up to 1 cm, as well as minor biotite and minor sulphides. Coarse and pegmatitic material occurs as indistinct pods and veinlets within finer-grained material and could be due to water-saturated crystallization. This would

also explain the presence of deuteric/primary biotite and amphibole in the samples. The biotite and amphibole are interpreted as deuteric/primary in origin because of the absence of any metamorphism that affected the sedimemtary rocks at this location.

Dyke Q/R: Finally, one sample (AX85-62) was selected from Dyke Q/R for Ar-40/Ar-39 whole rock dating. This 1.5 m thick dyke cuts Sill P, which is the uppermost sill of the series that was collected (See figure 6). Muecke noted that Dyke Q/R also cuts calcite veins within Sill P, indicating that Sill P cooled to a relatively low temperature before the intrusion of the cross-cutting dyke. By dating Dyke Q/R, a lower age limit (i.e. date of most recent activity) should be obtained for the Buchanan Lake magmatic activity. This is a slightly to moderately altered sample which is holocrystalline and porphyritic. Phenocrysts of olivine altered to iddingsite occur up to 1mm in size, and the matrix is generally <0.3 mm. The only high K-bearing phase present is altered interstitial glass.

Chapter 6. Ar-40/Ar-39 Results

The Ar-40/Ar-39 numerical results are listed in tables 5-14, and the age spectra and Ca/K diagrams for individual samples are displayed in figures 18-27.

Because of high atmospheric corrections mainly in the first and last outgassing steps, anomalies in the outer 5-10% of the Ar-39 release, of an otherwise concordant spectrum, are disregarded. In some cases, these anomalies may be due to diffusive argon loss (especially from chilled margins), excess argon incorporated into the crystal lattice, or recoil of reactor-produced Ar-39 from one phase to another during neutron irradiation.

6.1 Concordant Spectra

Three of the samples, from Tropical Ridge and Star Complex (See figures 18 -21),show essentially undisturbed whole rock spectra. The sample from Tropical Ridge (EL84-87), which shows moderate alteration, is concordant over 85% of the spectrum, with a plateau age of 93$\pm$2 Ma. The only disturbance occurs in the first 15%, and is therefore disregarded, as explained earlier. The low and consistent Ca/K ratios (2 to 4) over most of the range indicate that there is a high K phase, probably moderately altered

glass, which outgasses over most of the spectrum.

The two samples from Star Complex each yield plateau ages of 91±2 Ma over 85-90% of the spectra. EL84-50 is a pristine sample from the sill interior. It contains approximately 15% glass, which is the high K-bearing phase (2-3% K_2O with patches up to 7% K_2O), as confirmed by microprobe analysis (table 15). EL84-49, a highly altered sample from the chilled margin of the dyke, contains a considerable amount of devitrified glass and sericite, both high K-bearing phases, as well as interstitial carbonate (possibly calcite). As is commonly the case, the first 10% of this spectrum has been disturbed and therefore does not yield any geologically meaningful ages. From 20 to 65% Ar-39 released, the Ca/K diagram (See figure 19) shows a relatively high Ca/K ratio, probably due to the outgassing of calcite or another high Ca-bearing phase. Above 65%, the low Ca/K ratios are very similar to those discussed above, which were attributed to interstitial glass.

The spectra of samples EL84-87 and EL84-50 can be divided into three regions. In both cases, the first 15% of the spectra are discordant, the anomalies likely being due to extraneous argon or diffusive argon loss. The second region, characterized by low Ca/K ratios (between 2 and 4), covers

70% of the spectra. These low Ca/K ratios are attributed to glass, present in both samples. The third region occurs in the last 10-15% of the spectra. This is characterized by an increasing Ca/K ratio (from 4 to over 40) as well as a slight drop in apparent age (See figures 18 and 20). The anomalies in this final region are attributed to the outgassing of plagioclase at higher temperatures. The lowered ages due to the plagioclase are confirmed by sample EL84-50P, the felsic separate from sample EL84-50 (See figure 21). This sample displays an internally discordant Ar-40/Ar-39 age spectrum, in which no plateau is present and in which not one of the steps yields an apparent age above 73 Ma (c.f. 92 ± 2 and 91 ± 2 Ma for samples EL84-87 and EL84-50, respectively). This appears to indicate that plagioclase loses argon from its crystal lattice, even if there is no subsequent thermal disturbance.

The remaining concordant spectrum is from the Buchanan Lake samples. The most important is the biotite separate (AX85-218B; figure 27) which yields a plateau age of 126 ± 2 Ma over 90% of the spectrum. Its importance will be discussed in more detail later.

TABLE 5.

EL84-87 WHOLE ROCK SUMMARY

TEMP. (DEG.C)	mV Ar39	% Ar39	AGE (Ma)	% ATMOS.	Ar37/Ar39	% I.I.C.
			J = 2.4E-03			
200-500	2.7	3.4	95.6 +/- 1.6	80.5	1.6	.5
500-550	3.7	4.6	108.9 +/- .8	30	1	.3
550-600	5.9	7.3	100.6 +/- .5	20.2	.9	.2
600-650	7.2	8.9	95.2 +/- .4	25.5	.9	.3
650-700	9.8	12.2	93.4 +/- .4	24.3	1	.3
700-750	9.8	12.1	93.3 +/- .2	13.8	.9	.3
750-800	9.4	11.6	92.7 +/- .3	27.9	.8	.2
800-850	8.1	10.1	91.8 +/- .3	39.7	.7	.2
850-900	7.1	8.8	91.2 +/- .2	37.6	1.3	.4
900-950	5.5	6.8	90.8 +/- .6	49.1	2	.7
950-1000	5.3	6.6	90.7 +/- .7	58.9	3.2	1.2
1000-1050	3.5	4.3	88.8 +/- 1	76.9	7.5	3
1050-1100	1.7	2.1	88.7 +/- 2.5	87.1	15	6.2
1100-1150	.4	.5	100.3 +/- 30.9	96.7	31.5	11.9

TOTAL GAS AGE = 93.8 MY. +/- .7 MY. (.8 %)
TOTAL GAS AGE ABOVE 550°C = 93.0 MY.

% I.I.C. - INTERFERING ISOTOPES CORRECTION

ERROR ESTIMATES AT ONE SIGMA LEVEL

TABLE 6.

EL84-49 WHOLE ROCK SUMMARY

TEMP.(DEG.C)	mV Ar39	% Ar39	AGE(Ma)	% ATMOS.	Ar37/Ar39	% I.I.C.
			J = 2.4E-03			
200-500	4.2	3	55.6 +/- 1.4	91.9	4.1	2.5
500-550	7.1	5	82.3 +/- .4	44.6	4.2	1.8
550-600	4.5	3.2	89.2 +/- .3	23.7	2.2	.8
600-650	7.7	5.5	89.7 +/- .3	18.6	2.7	1
650-700	9.1	6.4	89.8 +/- .3	27.2	7	2.8
700-750	59	41.8	90.8 +/- .6	25.5	6.1	2.4
750-800	5.1	3.6	93 +/- .3	23.9	1.4	.5
800-850	3.9	2.7	90.5 +/- .4	27.3	1.2	.4
850-900	7.2	5.1	90.7 +/- .4	53.5	.8	.2
900-950	7.2	5.1	91.1 +/- .3	44.8	.6	.1
950-1000	8	5.7	90.9 +/- .3	40.7	.7	.2
1000-1050	5.7	4	91.3 +/- .6	50.5	1	.3
1050-1100	5.7	4	90.6 +/- .3	49.1	1.1	.4
1100-1150	6	4.3	89.5 +/- .6	63.6	2	.7

TOTAL GAS AGE = 89.2 MY. +/- .5 MY.(.6 %)
TOTAL GAS AGE ABOVE 550°C = 90.6 MY.

% I.I.C. - INTERFERING ISOTOPES CORRECTION

ERROR ESTIMATES AT ONE SIGMA LEVEL

TABLE 7.

EL84-50 WHOLE ROCK SUMMARY

TEMP.(DEG.C)	mV Ar39	% Ar39	AGE(Ma)	% ATMOS.	Ar37/Ar39	% I.I.C.
			J = 2.4E-03			
200-500	30	15.6	64.3 +/- 1.3	86.2	1	.4
500-550	3.5	1.8	95.6 +/- .8	58.7	.9	.3
550-600	3.9	2	94.9 +/- .5	55.6	1	.3
600-650	3.1	1.6	90.6 +/- .9	60.1	1.6	.6
650-700	4.8	2.5	90.9 +/- .5	57.1	2	.7
700-750	41.9	21.9	93.2 +/- .5	53.5	1.7	.6
750-800	5	2.6	91.3 +/- .5	58.5	1.4	.5
800-850	5.1	2.7	89.8 +/- .7	71.6	1.1	.4
850-900	29	15.1	90 +/- 1	67.9	1.4	.5
900-950	34	17.7	89.4 +/- .7	68	2	.7
950-1000	25	13	88.9 +/- 1.1	69.5	2.3	.8
1000-1050	3.2	1.6	88.8 +/- 1.3	74.5	4.4	1.8
1050-1100	1.8	.9	84.8 +/- 2.2	86.4	12.1	5.2
1100-1150	.5	.2	68 +/- 37.9	97.8	41.3	21.9

TOTAL GAS AGE = 86.6 MY. +/- 1 MY.(1.2 %)
TOTAL GAS AGE ABOVE 550°C = 90.0 MY.

% I.I.C. - INTERFERING ISOTOPES CORRECTION

ERROR ESTIMATES AT ONE SIGMA LEVEL

TABLE 8.

EL84-50P FELSICS SUMMARY

TEMP.(DEG.C)	mV Ar39	% Ar39	AGE(Ma)	% ATMOS.	Ar37/Ar39	% I.I.C.
			J = 2.52E-03			
200-500	.4	3.7	-72.6 +/- -32.5	106.1	5.5	2.2
500-550	.3	3.6	3.5 +/- 17.4	99.3	7.7	73.4
550-600	.5	5.2	25.2 +/- 6.4	90.3	9.2	12.7
600-650	.8	7.8	52.7 +/- 8.7	78.1	10.5	7.2
650-700	1.2	11.6	59.3 +/- 1.8	74.2	11.2	6.9
700-750	1.5	14.6	65.1 +/- 2.1	73.5	11.1	6.3
750-800	1.2	11.3	66.2 +/- 2.5	78.5	10.8	6
800-850	1	9.8	73.2 +/- 4.8	84.3	10.2	5.2
850-900	.6	6.1	39.4 +/- 12.9	95	8.4	7.5
900-950	.4	4.3	7.6 +/- 21.3	99.4	7.1	31.1
950-1000	.2	2.8	5.2 +/- 18.3	98.9	7.2	45.8
1000-1050	1.2	11.2	64.1 +/- 10	93.2	9.4	5.4
1050-1150	.8	7.5	54 +/- 10.5	95.5	13.1	8.9

TOTAL GAS AGE = 48.4 MY. +/- 6 MY.(12.5 %)
TOTAL GAS AGE ABOVE 550°C = 60.7 MY.

% I.I.C. - INTERFERING ISOTOPES CORRECTION

ERROR ESTIMATES AT ONE SIGMA LEVEL

TABLE 9.

AX85-62 WHOLE ROCK SUMMARY

TEMP.(DEG.C)	mV Ar39	% Ar39	AGE(Ma)	% ATMOS.	Ar37/Ar39	% I.I.C.
			J = 2.4E-03			
200-500	1.7	7.3	67.3 +/- 5.4	94.5	3.9	2
500-550	1.2	5.2	128.4 +/- 3.7	83	3.5	1
550-600	1.5	6.4	129.6 +/- 3.1	81.8	4.4	1.3
600-650	1.7	7	79.3 +/- 4.5	88.9	7.7	3.5
650-700	1.9	7.9	101.5 +/- 1.9	80.3	7.1	2.6
700-750	3.4	14.1	113.4 +/- 1.2	71.9	4.7	1.5
750-800	3.9	16.4	114.2 +/- 1.5	75.6	3.7	1.2
800-850	2.1	8.7	110.8 +/- 2.3	84.4	3.4	1.1
850-900	1.8	7.5	116.1 +/- 2.4	77.4	3.4	1.1
900-950	1.3	5.7	88.3 +/- 3.5	86	4.9	2
950-1000	1.3	5.3	84.4 +/- 3.2	88.4	7.6	3.3
1000-1050	.9	3.8	81.9 +/- 5.9	90.8	13.7	6.1
1050-1100	.6	2.6	68.2 +/- 10.1	95.6	41	21.7
1100-1150	.3	1.4	58.6 +/- 68.8	98.5	123.3	75.1

TOTAL GAS AGE = 102.5 MY. +/- 4.1 MY. (4 %)
TOTAL GAS AGE ABOVE 550°C = 104.4 MY.

% I.I.C. - INTERFERING ISOTOPES CORRECTION

ERROR ESTIMATES AT ONE SIGMA LEVEL

TABLE 10.

AX85-215 WHOLE ROCK SUMMARY

TEMP. (DEG.C)	mV Ar39	% Ar39	AGE (Ma)	% ATMOS.	Ar37/Ar39	% I.I.C.
			J = 2.4E-03			
200-500	2	3.3	34.2 +/- 4.2	97.2	2.5	2.3
500-550	15	24.3	64.2 +/- 1.6	87.8	1.9	.9
550-600	1.7	2.8	101.2 +/- 2.1	80.9	1.8	.6
600-650	1.9	3.1	100.9 +/- 2.1	78.6	2.4	.8
650-700	2.8	4.7	108.2 +/- 1.3	69	2	.6
700-750	2	3.3	104.2 +/- 2	65.3	1.4	.4
750-800	2.4	4	111.4 +/- 1.3	72.5	1.4	.4
800-850	4.2	6.9	106.9 +/- .8	72.7	.9	.2
850-900	7.5	12.2	114.1 +/- .5	55	1.1	.3
900-950	12.4	20.1	112.4 +/- .2	39.6	1.4	.4
950-1000	4.5	7.4	97.6 +/- .6	56.8	3.7	1.3
1000-1050	1.9	3.1	89.6 +/- 2	85	11.6	4.8
1050-1100	1.6	2.6	114.2 +/- 3.8	86.5	20.3	6.8
1100-1150	.9	1.4	118.5 +/- 8.8	93.1	27.4	9

TOTAL GAS AGE = 95.2 MY. +/- 1.4 MY. (1.5 %)
TOTAL GAS AGE ABOVE 550°C= 108.2 MY.

% I.I.C. - INTERFERING ISOTOPES CORRECTION

ERROR ESTIMATES AT ONE SIGMA LEVEL

TABLE 11.

AX85-217P FELSICS SUMMARY

TEMP.(DEG.C)	mV Ar39	% Ar39	AGE(Ma)	% ATMOS.	Ar37/Ar39	% I.I.C.
			J = 2.52E-03			
200-500	1.2	3.5	330.1 +/- 3.9	69.4	3.8	.5
500-550	1.5	4.6	114.9 +/- 2.8	79.1	4.2	1.4
550-600	1.1	3.2	202.6 +/- 2.4	57.3	6.7	1.4
600-650	2.2	6.6	130.6 +/- 1.3	62.7	9.6	2.9
650-700	2.1	6.4	102.8 +/- 1.3	64.2	9.8	3.7
700-750	1.7	5.1	120.1 +/- 2	67.4	5.2	1.7
750-800	1.8	5.5	124.7 +/- 2	67.4	3.8	1.2
800-850	3.3	9.9	119.9 +/- 1.1	62.8	2.4	.7
850-900	4	12	128.4 +/- .9	53.7	1.7	.5
900-950	3.6	10.8	119.8 +/- 1	55.4	1.9	.6
950-1000	2.9	8.8	115.9 +/- 1	57.7	2.4	.8
1000-1050	3.4	10.1	139.1 +/- 1.2	59.1	3.9	1.1
1050-1100	2.3	7	170.4 +/- 1.3	50.7	4	.9
1100-1140	2	6	189.2 +/- 2	60.1	3.8	.8

TOTAL GAS AGE = 140.7 MY. +/- 1.6 MY.(1.1 %)
TOTAL GAS AGE ABOVE 550°C = 134.1 MY.

% I.I.C. - INTERFERING ISOTOPES CORRECTION

ERROR ESTIMATES AT ONE SIGMA LEVEL

TABLE12.

AX85-217M MAFICS SUMMARY

TEMP.(DEG.C)	mV Ar39	% Ar39	AGE(Ma)	% ATMOS.	Ar37/Ar39	% I.I.C.
			J = 2.52E-03			
200-500	1.5	11.3	49.1 +/- 7.1	95.7	2.2	1.5
500-550	.9	6.8	55.5 +/- 5.1	92.9	1.5	.9
550-600	.8	6.4	145.3 +/- 11.9	89.2	2.7	.7
600-650	.3	3	142.7 +/- 22.4	90.2	3.9	1.1
650-700	.6	4.7	125.6 +/- 12.7	89.7	3	.9
700-750	1.1	8.6	136.5 +/- 4.8	82.4	1.9	.5
750-800	1.4	11.2	133.5 +/- 3	79.5	1.7	.4
800-850	1.2	9.3	147.7 +/- 2.9	72.6	2.1	.5
850-900	2	15.8	132.9 +/- 3.6	77.9	2.1	.6
900-950	1.3	9.8	124.1 +/- 2.4	79.7	4.1	1.3
950-1000	1	8	110.6 +/- 3.5	80.7	6.2	2.2
1000-1050	.3	2.9	113.9 +/- 40	93.5	15.4	5.4
1050-1100	.2	1.6	163.6 +/- 95	96	48.8	12.8

TOTAL GAS AGE = 118.2 MY. +/- 8.6 MY.(7.3 %)
TOTAL GAS AGE ABOVE 550°C = 132.6 MY.

% I.I.C. - INTERFERING ISOTOPES CORRECTION

ERROR ESTIMATES AT ONE SIGMA LEVEL

TABLE 13.

AX85-218P FELSICS SUMMARY

TEMP.(DEG.C)	mV Ar39	% Ar39	AGE(Ma)	% ATMOS.	Ar37/Ar39	% I.I.C.
			J = 2.52E-03			
500-550	1.3	4.8	0 +/- 0	0	0	0
500-550	2.3	8.2	87.7 +/- 1.1	42.8	1.6	.6
550-600	2.1	7.5	113 +/- 1.2	42.7	3.1	1
600-650	2	7	131.1 +/- 1	36.4	5.2	1.6
650-700	2.1	7.3	104.9 +/- 1.3	34.4	5.4	2
700-750	2	7.2	123.4 +/- 1.2	31.1	4	1.3
750-800	1.6	5.7	119.9 +/- 2	48	3.3	1
800-850	1.6	5.8	128.4 +/- 2.7	45.4	2.2	.6
850-900	1.7	5.9	139.1 +/- 1.6	48.3	1.5	.4
900-950	1.9	6.6	143.8 +/- 1.3	49.6	1.5	.3
950-1000	2.4	8.5	129.5 +/- 1	52.9	1.7	.5
1000-1050	1.9	6.6	138.2 +/- 1.1	50.6	1.5	.4
1050-1100	3.4	11.9	151.3 +/- 1.8	40.9	1.1	.2
1100-1150	1.8	6.3	162.2 +/- 2.3	58.2	1.7	.4

TOTAL GAS AGE = 128.9 MY. +/- 1.6 MY.(1.2 %)
TOTAL GAS AGE ABOVE 550°C = 132.7 MY.

% I.I.C. - INTERFERING ISOTOPES CORRECTION

ERROR ESTIMATES AT ONE SIGMA LEVEL

TABLE 14.

AX85-218B BIOTITE SUMMARY

TEMP.(DEG.C)	mV Ar39	% Ar39	AGE(Ma)	% ATMOS.	Ar37/Ar39	% I.I.C.
			J = 2.52E-03			
200-550	15.8	6.1	62.5 +/- 2.1	82.8	0	.1
550-650	14.4	5.5	118.7 +/- 1.8	68.1	0	0
650-700	12.6	4.8	122.6 +/- 2.1	62.5	0	0
700-750	19	7.3	123.8 +/- 1.4	63.1	0	0
750-800	17.6	6.8	124.9 +/- 1.5	67.2	0	0
800-850	26.6	10.2	128.9 +/- .8	54.7	0	0
850-900	79	30.4	129.5 +/- .4	27.7	0	0
900-950	68.2	26.3	125.2 +/- .3	31.2	0	0
950-1000	5.5	2.1	122.8 +/- 8.3	85	0	0

TOTAL GAS AGE = 122.4 MY. +/- 1.1 MY.(.9 %)
TOTAL GAS AGE ABOVE 550°C = 126.3 MY.

% I.I.C. - INTERFERING ISOTOPES CORRECTION

ERROR ESTIMATES AT ONE SIGMA LEVEL

FIGURE 18 EL84-87WR

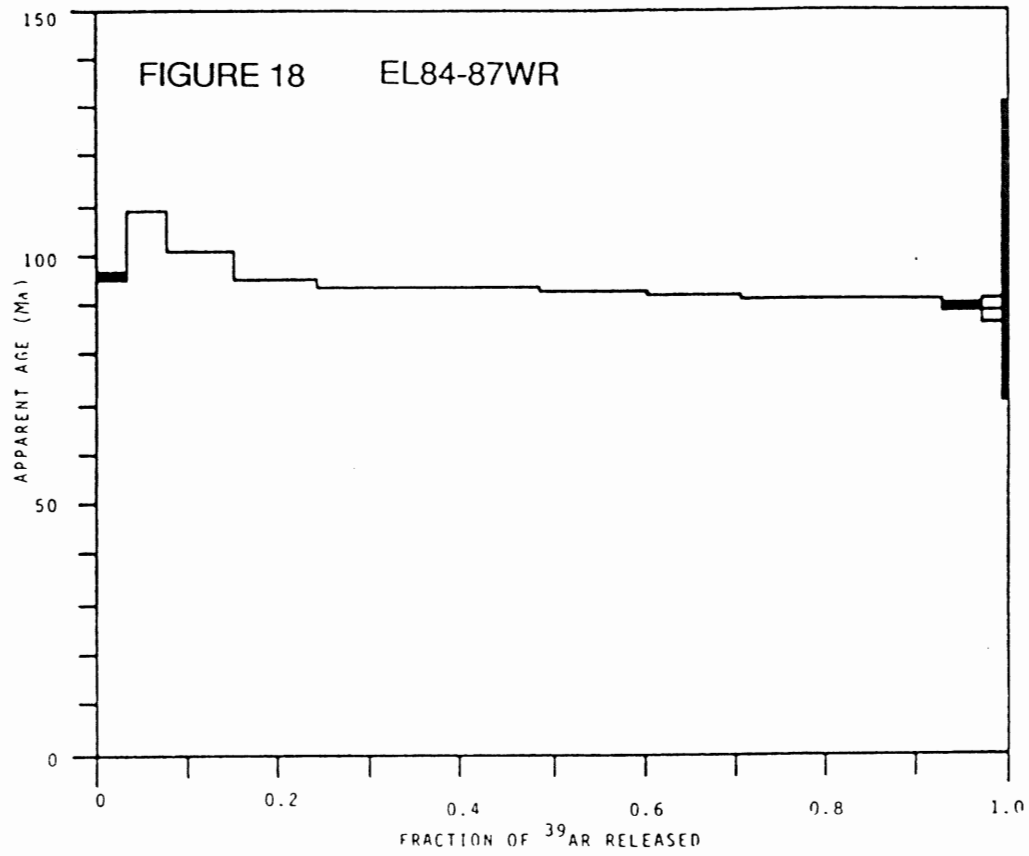

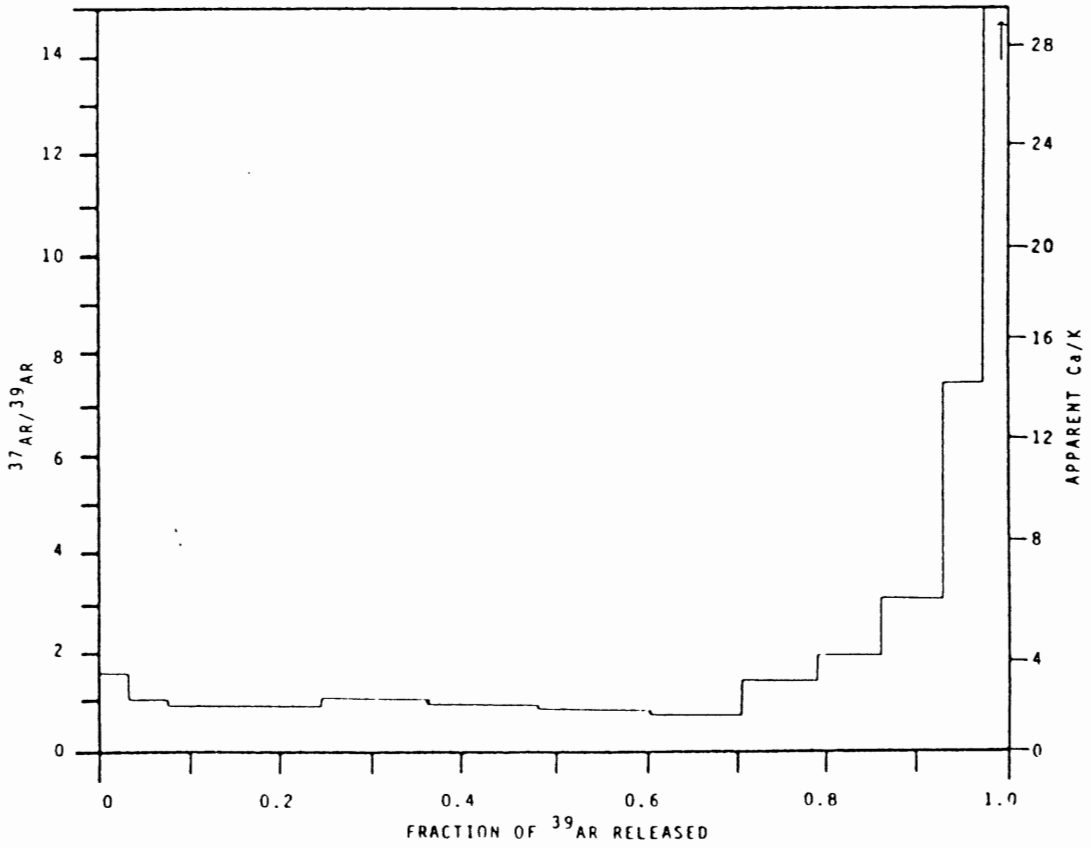

FIGURE 19 EL84-49WR

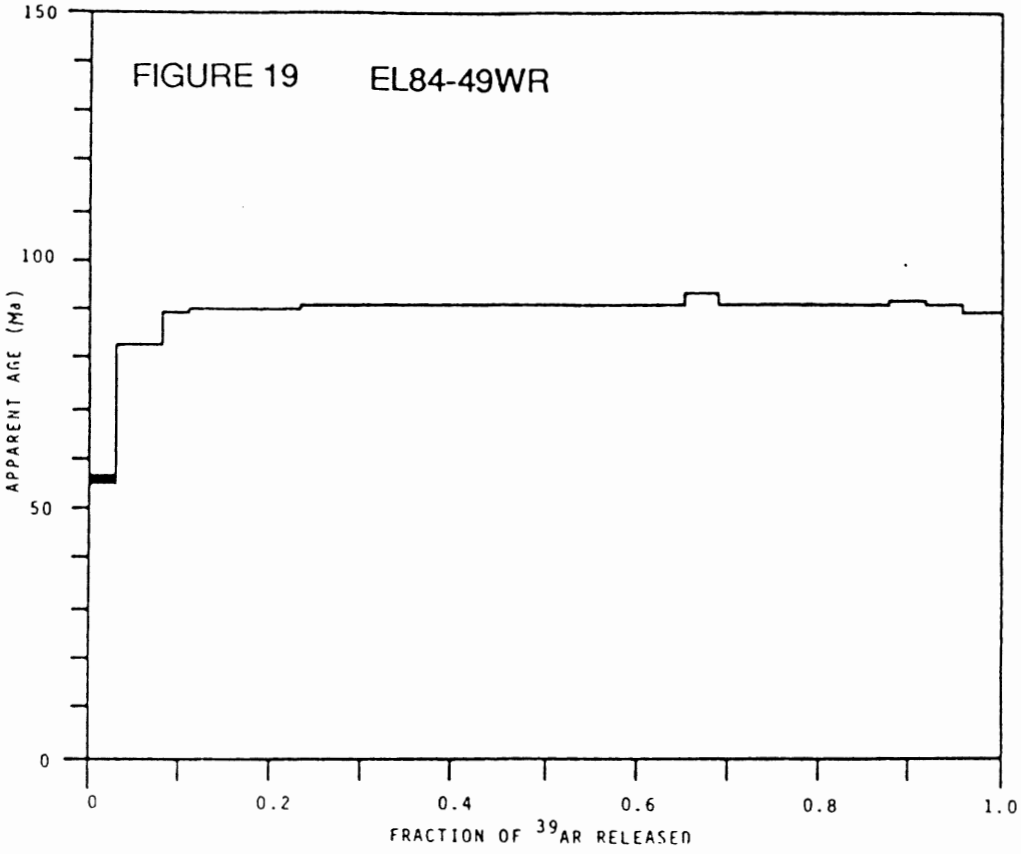

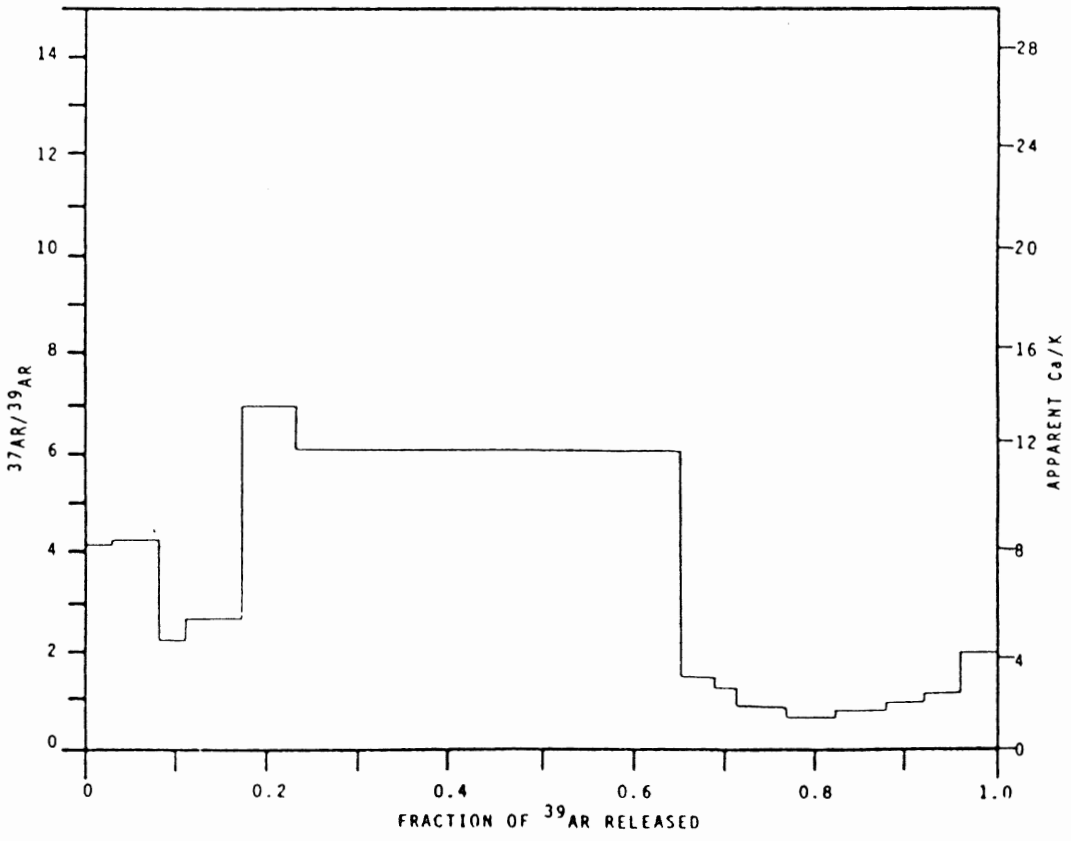

FIGURE 20 EL84-50WR

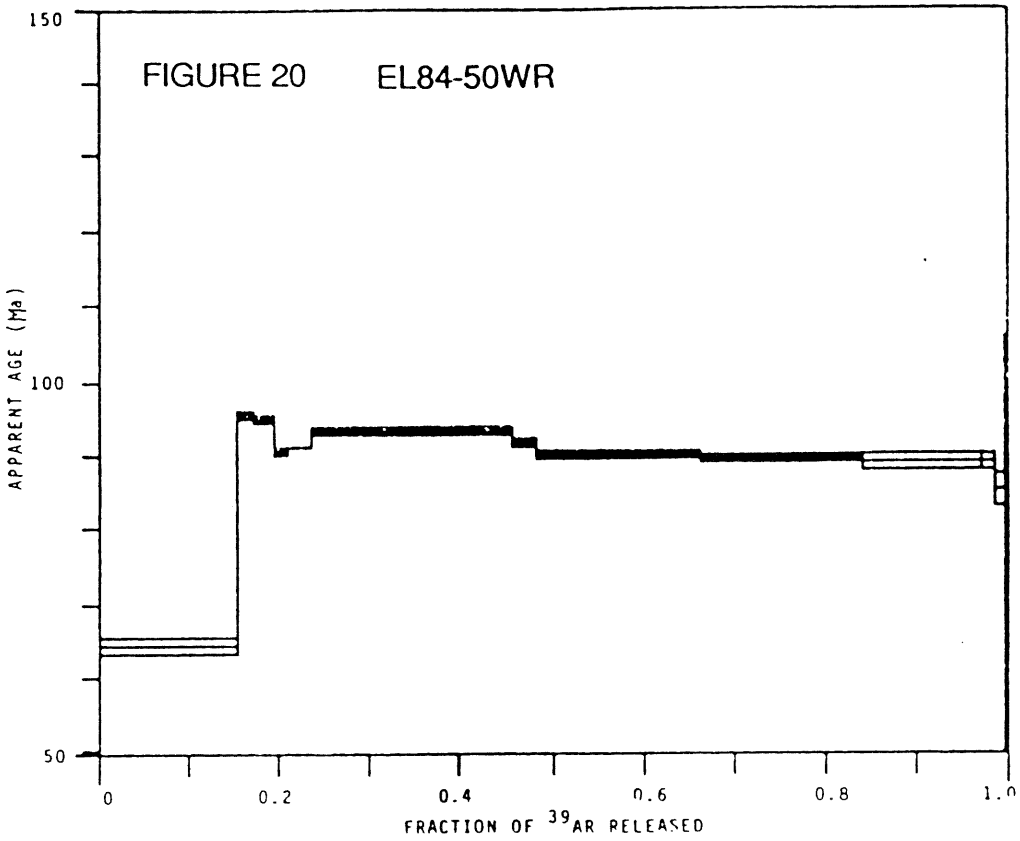

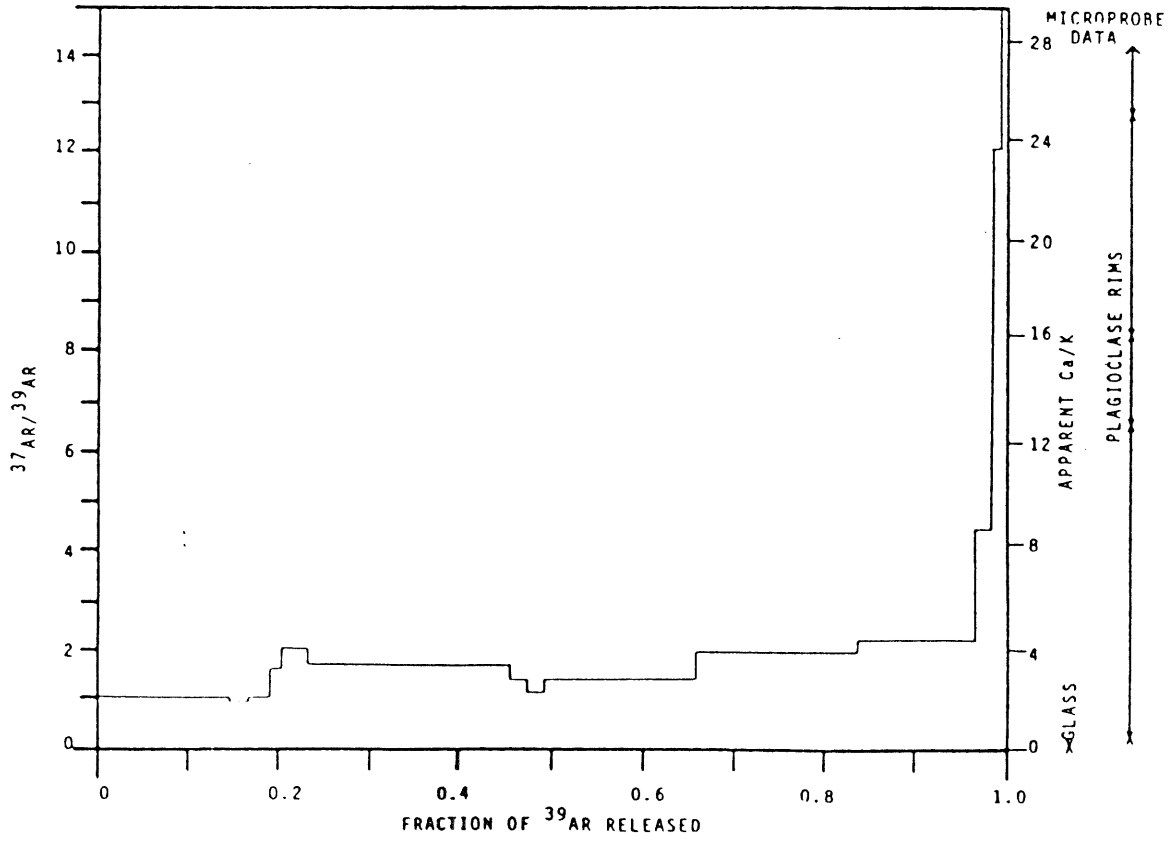

FIGURE 21 EL84-50P

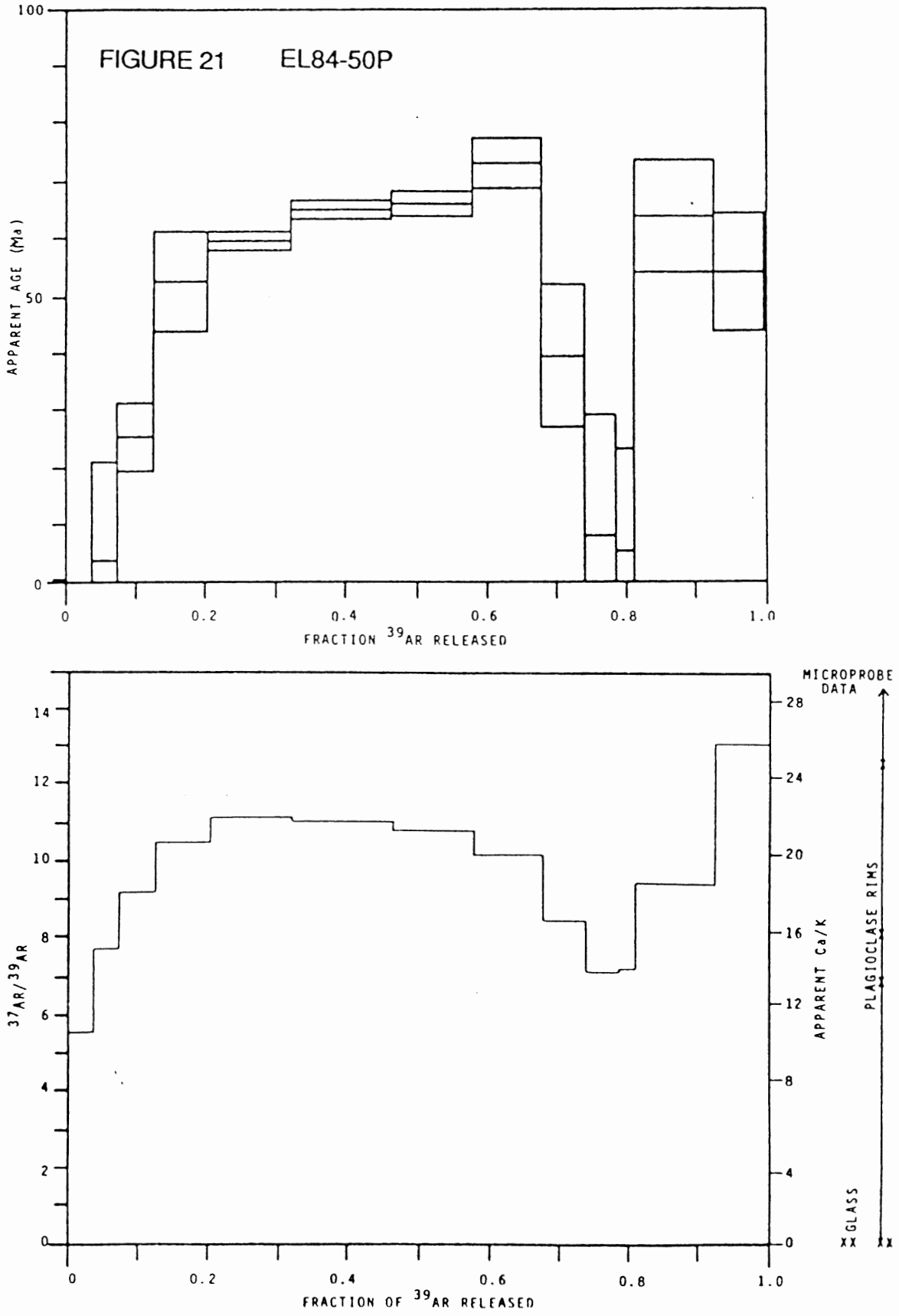

FIGURE 22 AX85-62WR

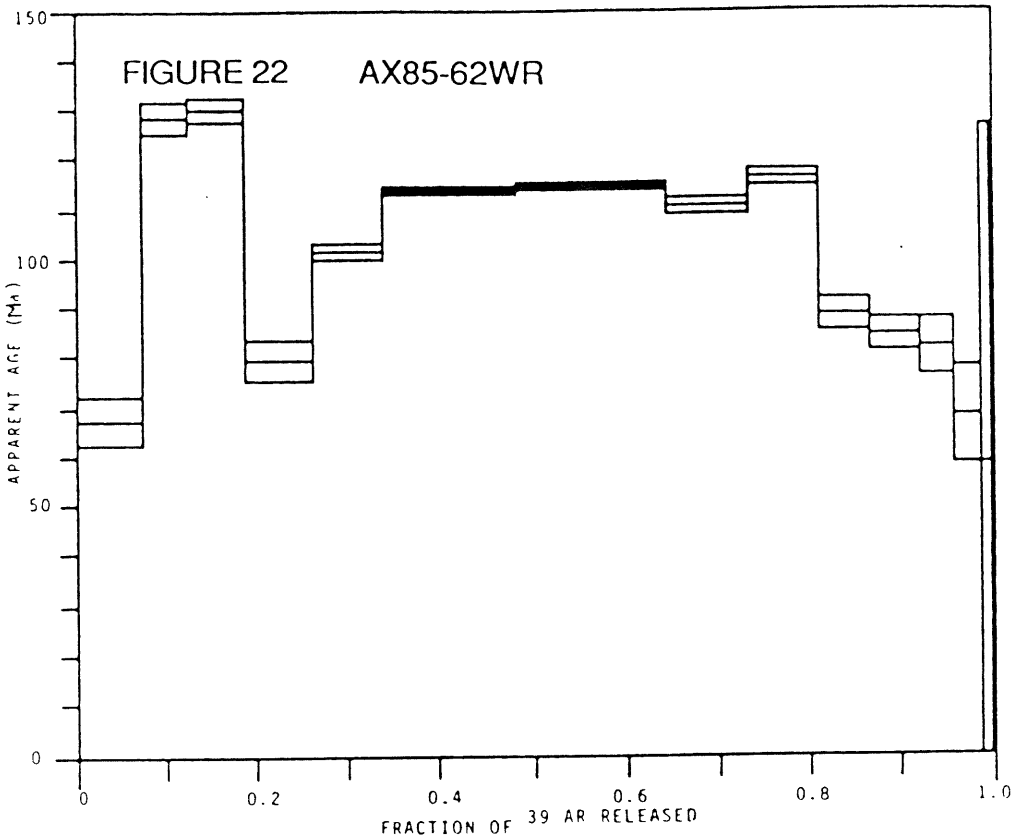

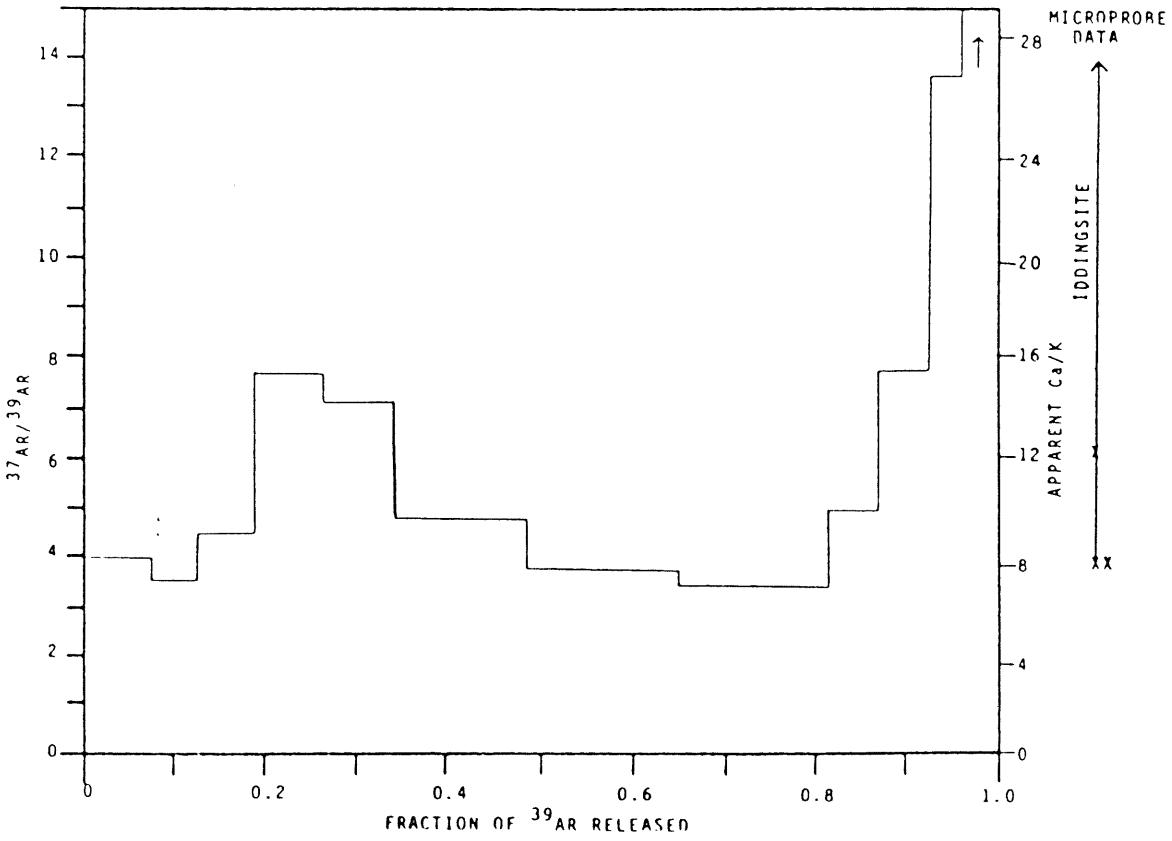

FIGURE 23 AX85-215WR

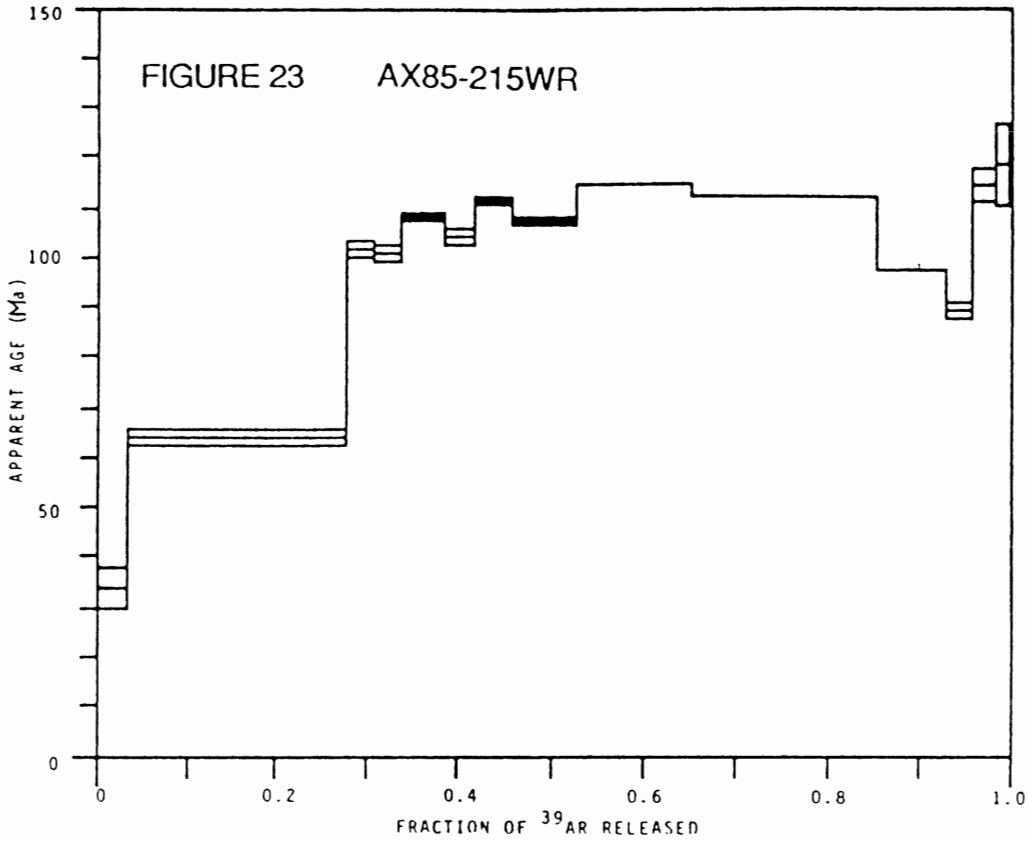

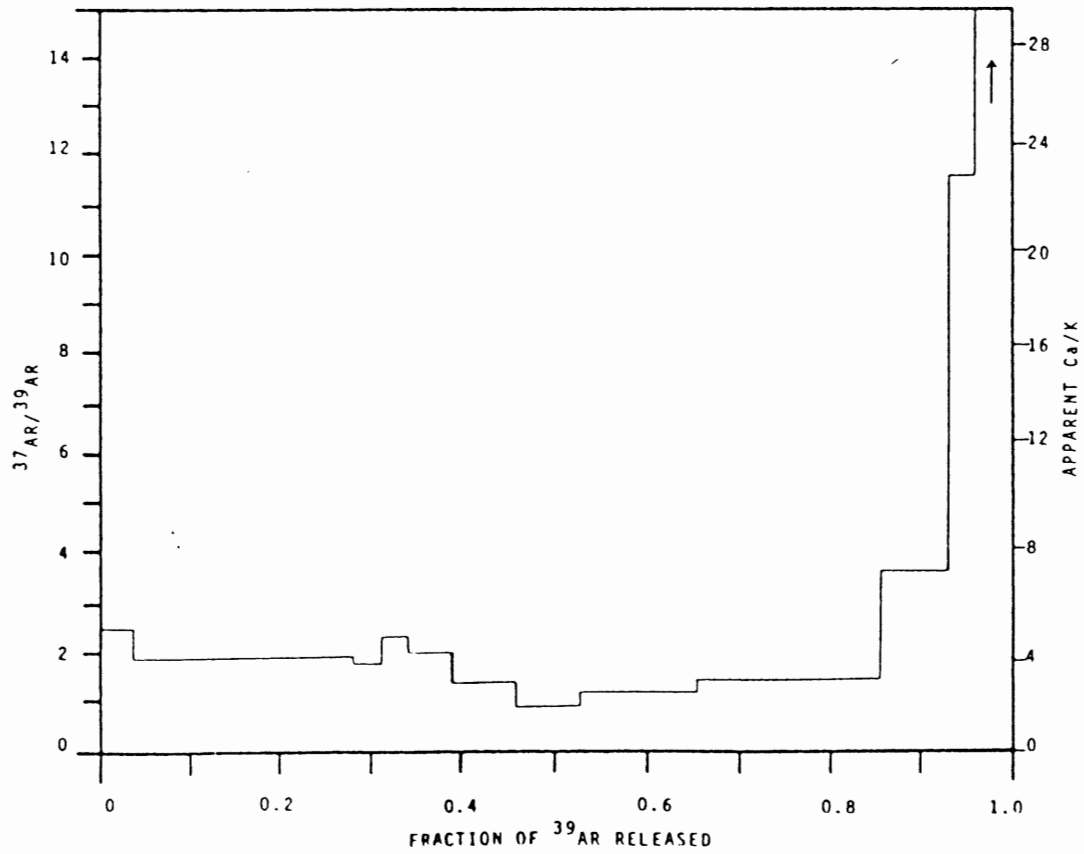

FIGURE 24 AX85-217P

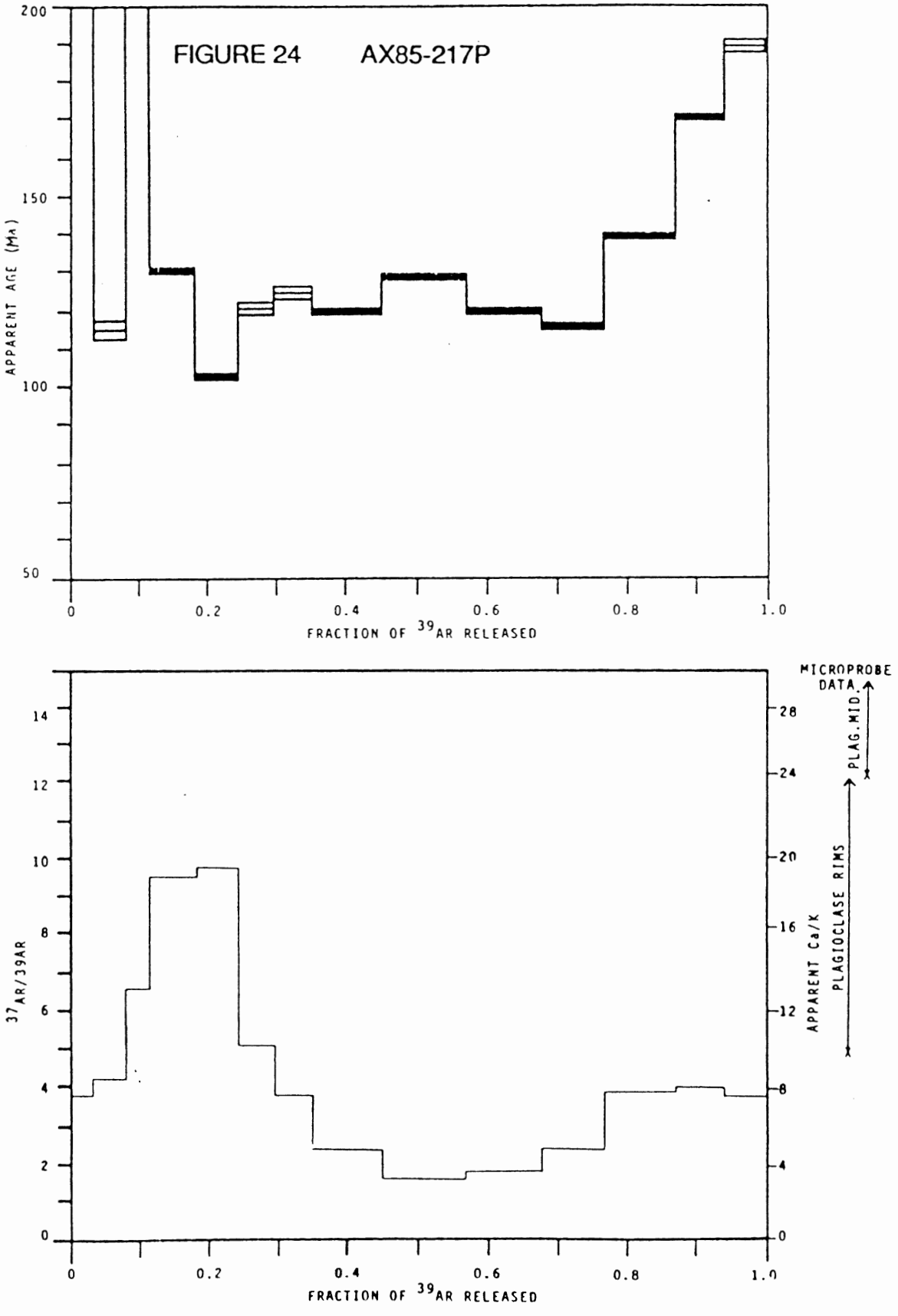

FIGURE 25 AX85-217M

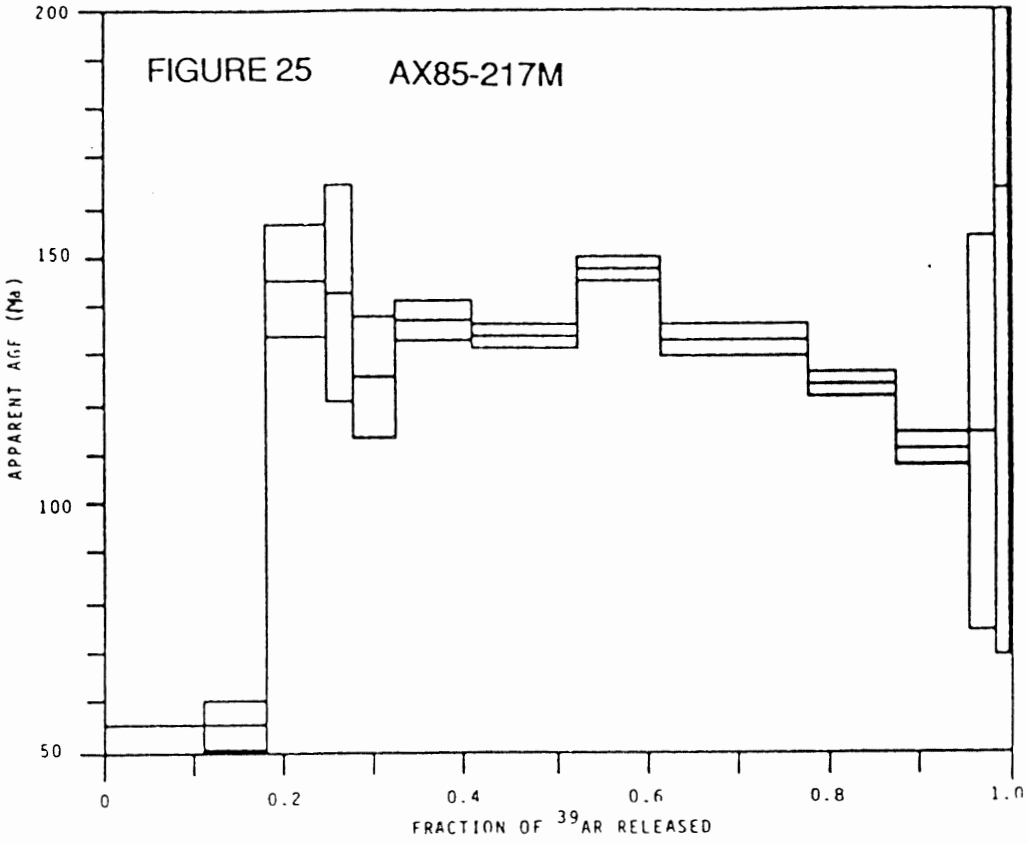

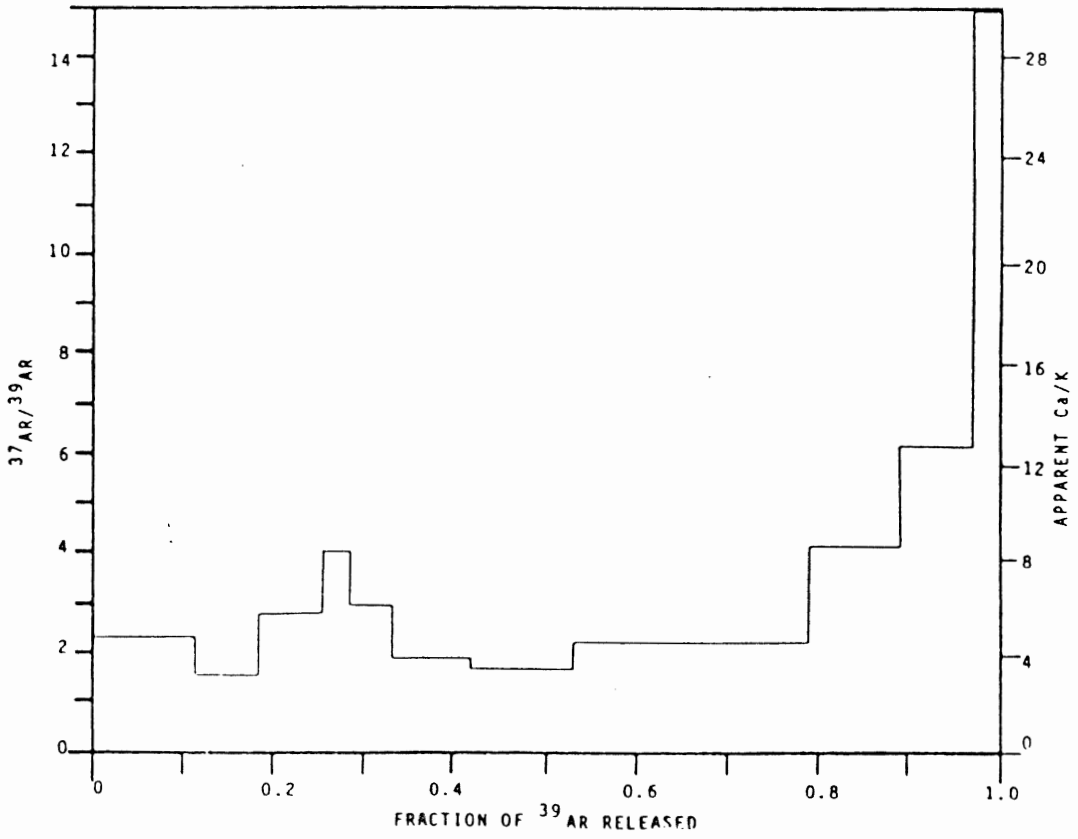

FIGURE 26 AX85-218P

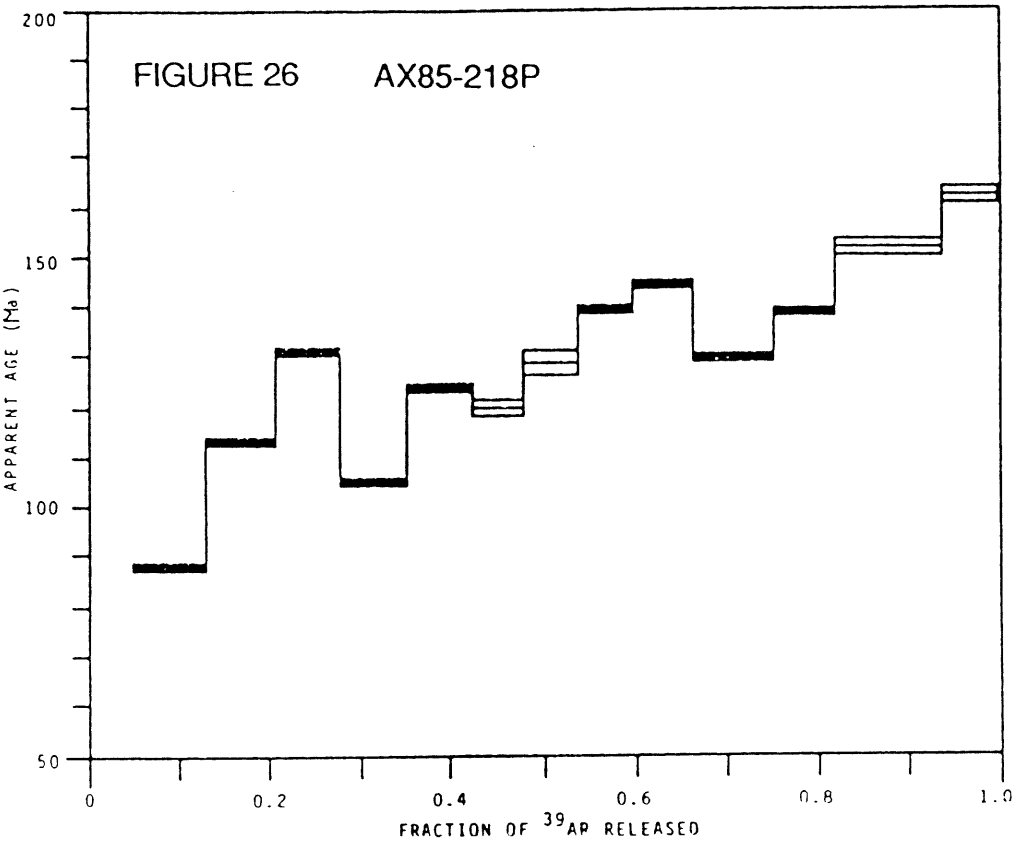

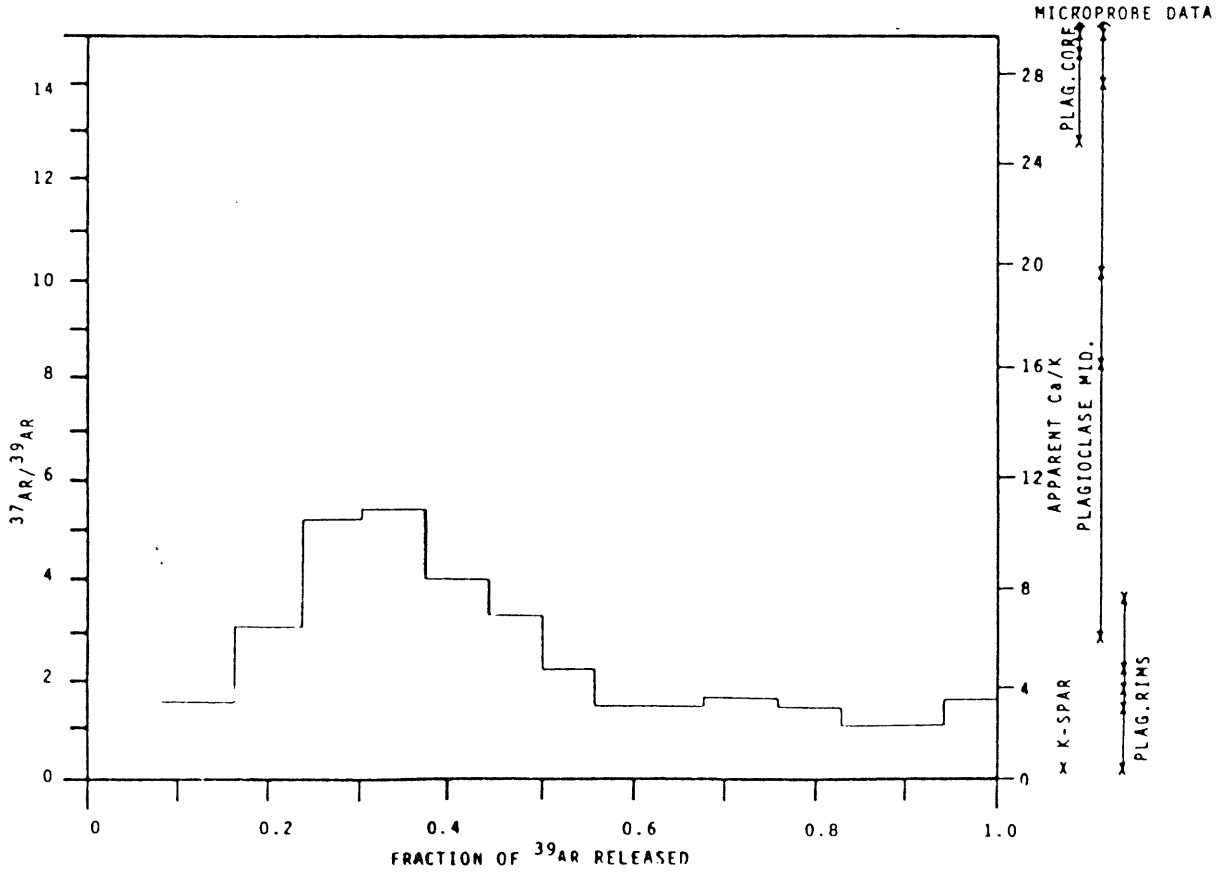

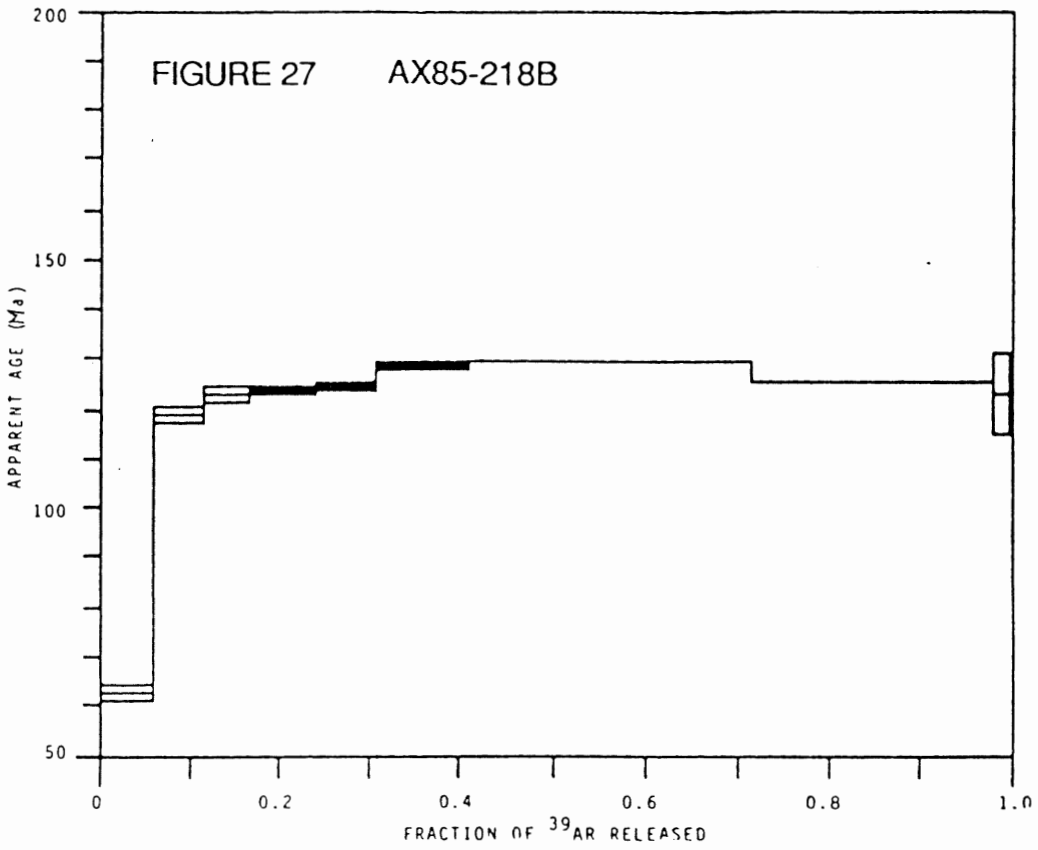
FIGURE 27
AX85-218B
200
150
100
50
APPARENT AGE (Ma)
0
0.2
0.4
0.6
0.8
1.0
FRACTION OF ^{39}AR RELEASED

6.2. Discordant Spectra

The whole rock spectra are from Sill A (AX85-215; figure 23) and a cross-cutting Dyke Q/R (AX85-62; figure 22), both finely crystalline samples. The spectra derived from these two samples appear to show both intrinsic similarities and differences. Sample AX85-215 contains approximately 20% biotite and sericite, both high K-bearing phases, while the only obvious K-bearing phases in sample AX85-62 are minor sericite and altered glass. Apart from an anomalously high apparent age in the second and third steps of the latter sample, these two spectra coincide quite closely when superimposed. If the anomaly, possibly due to a "catcher phase" of high argon retentivity or excess argon, is disregarded, the degree of agreement between these two spectra is comparable to that of the duplicate runs of one sample carried out by Zeitler and Fitz Gerald (1986) (See Figure 28). The high temperature decreases in apparent age probably correspond to the outgassing of plagioclase, as explained earlier (refer to section 6.1.). This similarity seems to indicate that these two bodies have had similar thermal histories since the time of dyke emplacement.

An alternate treatment of these spectra takes into account the different Ca/K ratios, despite the spectral similarities. In this case, rather

than identifying a high apparent age anomaly in the second and third steps of the spectrum, a low apparent age anomaly in the fourth and fifth steps is identified. The latter anomaly corresponds to the outgassing of a phase with a high Ca/K ratio (See figure 22). If this is the correct treatment, then the two spectra are not as similar as they first appear (i.e. the first 30%of the spectra become quite distinct). With the data available, it is not clear which of the above treatments is valid.

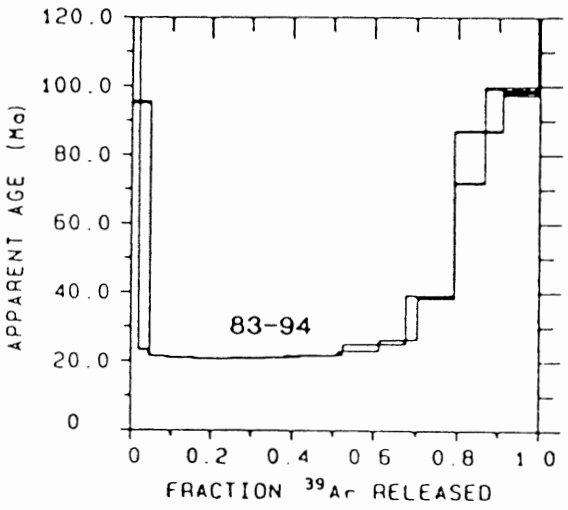

Figure 28. Ar-40/Ar-39 Age spectrum plot showing duplicate runs of a single feldspar separate. (After Zeitler and Fitz Gerald, 1986)

The three remaining spectra, all from Sill A, also fall into the category of discordant spectra; but nevertheless may contain useful information. Sample AX85-218P is a felsic fraction dominated by K-feldspar. The latter was confirmed by microprobe analysis which aided in

identifying orthoclase in a granophyric intergrowth with quartz. This spectrum resembles a staircase, a typical spectrum when internal argon redistribution has occurred (Bottomley and York, 1976) (See figure 26). Sometimes these spectra can be integrated to give useful ages, and it seems that for this sample, that treatment is valid. The total fusion age of 129±2 Ma (See table 11) is in agreement with the biotite age for the same sample (126±2 Ma).

Alternate interpretations of this spectral shape include slow cooling, the highest temperature step yielding the time of onset of crystallization; and reheating, the lowest temperature step yielding the time of thermal disturbance (Harrison and McDougall, 1982; Reynolds et al, in prep). Based on the information obtained from the biotite spectrum, both of these explanations can be discounted. The slow cooling scenario does not conform well because the high temperature age is considerably older than that indicated by the biotite spectrum. If anything, the biotite age should be older, because it begins to retain argon at a higher temperature (300° to 350°C) than do feldspars (200° to 250°C) (York,1984). The reheating scenario does not conform well because, although the low temperature age of ca. 90 Ma could correspond to a later thermal disturbance, the high

temperature age is again too high, for the reasons noted above.

The spectrum for sample AX85-217P is saddle-shaped, typical of minerals containing excess argon (See figure 24). This spectrum begins at a very high age, drops to a broad, though not particularly concordant, minimum at 115±10 Ma, and then rises again. It has been shown (Stukas and Reynolds, 1974; Zeitler and Fitz Gerald, 1986) that minimum saddle ages can give useful ages, and that seems to be the case with this sample. The mafic spectrum, sample AX85-217M, starts at low ages, rises to a broad maximum at 130±10 Ma, and then falls off again (See figure 25). Just as the minimum of the saddle-shaped felsic spectrum coincided with the biotite age (126±2 Ma), so does the maximum of the inverted-saddle-shaped mafic spectrum (120±10 Ma). It must be stated, however, that given only the mafic or the felsic spectrum, and relying on present understanding of complex spectra, a precise and accurate age could not be obtained with significant certainty.

In all cases in which the plagioclase crystals were zoned (labradorite cores, andesine/oligoclase rims), the potassium tended to concentrate toward the rims, a typical rim composition being 0.9% K_2O, and a typical core composition being <0.2% K_2O. (See table 15).

6.3. Ca/K Ratio Calculations

An attempt was made to correlate the Ca/K ratios of particular mineral phases derived from microprobe data with the ratios of individual Ar-40/Ar-39 outgassing steps. This was carried out as follows:

1) The standard hornblende, MMhb-1, has a Ca/K ratio of 4.73 (Roddick, 1983)

2) The average Ar-37/Ar-39 ratio calculated from 19 samples from 3 irradiation canisters is 2.42 (Reynolds, pers. com.).

3) By dividing the Ca/K ratio by the Ar-37/Ar-39 ratio, a correction factor, b, can be derived, and the Ca/K ratio of each outgassing step can be determined.

$$Ca/K = b \times (Ar\text{-}37/Ar\text{-}39) \; ; \quad \text{in this case, } b=1.95$$

From the data obtained (See figures 18-27 and table 15), no quantitative correlation between the microprobe data and the Ar-40/Ar-39 data is apparent; although samples which contained higher-K phases did show lower Ca/K ratios overall, as expected.

6.4. Summary of Ar-40/Ar-39 Dates

A summary of the age estimates is given in the following table (15):

Table 15.

Tropical Ridge	EL84-87WR	92±2 Ma
Star Complex, Dyke/Sill #4	EL84-49WR	91±2 Ma
	EL84-50WR	91±2 Ma
	EL84-50P	?
Buchanan Lake, Dyke Q/R	AX85-62WR	113±6 Ma
Sill A	AX85-215WR	112±6 Ma
	AX85-217P	120±10 Ma
	AX85-217M	130±10 Ma
	AX85-218P	129±2 (total fusion)
	AX85-218B	126±2

Table 16. Ca/K (wt/wt) Ratios from Selected Phases

(Microprobe Data)

Sample EL84-50

Plagioclase

	Core	Core	Mid1	Mid2	Rim	Rim
1.	69	46	161	68	75	---
2.	52	68	63	40	16	25
3.	44	41	51	70	13	---

Glass

1.	0.17	4.	0.11	7.	0.17
2.	0.017	5.	0.14	8.	0.18
3.	0.11	6.	0.062	9.	0.073

Sample AX85-62

Iddingsite/Chlorophaeite

1.	8
2.	13
3.	8
4.	34

Sample AX85-217

Plagioclase

	Core	Core	Mid1	Mid2	Rim
1.	64	42	54	64	51
2.	49	103	77	24	10
3.	128	47	94	35	39

Hornblende

1.	394	4.	87
2.	1263	5.	88
3.	43		

Sample AX85-218

Plagioclase

	Core	Core	Mid1	Mid2	Rim	Rim
1.	30	33	30	5.7	2.6	---
2.	25	29	20	16	7.6	---
3.	52	36	43	27	3.7	4.8

Orthoclase

1.	0.01
2.	0.04
3.	0.004
4.	0.02

Biotite

1.	0
2.	0.007
3.	0.006

Chapter 7. Interpretation of Results

7.1. Spectral Interpretation

Prior to experimentation, it was expected that the biotite separate would produce the best spectrum, because of its simple chemistry and its argon-retention properties. Next to the biotite separate the mafic and felsic fractions were expected to yield reliable results, because of their relatively simple compositions. The whole rock fractions were not expected to yield simple spectra, primarily because of their complex mineralogy and alteration history; but this was not the case. In general, whole rock samples gave spectra which were much more concordant than the mafic or felsic fractions, with the exception of the biotite fraction. The biotite phase probably formed by deuteric alteration during cooling and has remained unaltered since that time. It is assumed to give the "correct" age of the earlier intrusion, and is therefore seen as a reference. Although interpretation of the more complex spectra may be somewhat contentious, or even impossible, it is believed that these spectra are characteristic of particular minerals in a given environment, and do reflect the thermal histories of the samples (York,1984).

The Ar-40/Ar-39 spectra obtained from the older intrusions indicate

that these rocks were thermally disturbed by the younger intrusions, but their spectra were not entirely overprinted (i.e. reliable ages can still be derived). The younger whole rock samples yielded excellent plateau spectra, indicating that they have been undisturbed since the time of emplacement.

The three samples (EL84-87,EL84-49, and EL84-50) apparently belong to the latest episode of igneous activity in the Sverdrup Basin (late Cenomanian/early Turonian), as no later dates have been obtained in the area. They all contain about 10% glass or altered glass and give plateau ages despite differing degrees of alteration. This indicates that thermal disturbance, rather than degree of alteration, is the main cause of complex spectra. Because of this, samples may be chosen for dating without the need for particular regard for sample alteration per se; but it is important, if the alteration products are high K-bearing phases, that the alteration occurred soon after the time of emplacement and led to the production of secondary minerals with a good ability to retain argon. Otherwise, the date obtained from the sample could be the age of late alteration. For this reason, deuteric or automorphic phases such as biotite (AX85-218B) or amphibole, which are not overprinted by low temperaature (<250°C) disturbances (York,1984), give the most reliable dates. Samples which contain glass,

usually a very high K-bearing component of the rock, also yield reliable dates. This is because even a moderate amount of argon loss, quantitatively, is apparently insignificant relative to the amount of argon remaining in the rock. The mafic and felsic fractions (EL84-50P, AX85-217P, AX85-217P, AX85-218P) all display internally discordant Ar-40/Ar-39 spectra, from which reliable dates of intrusion cannot be obtained.

A point of particular interest about sample AX85-215 is that the total fusion age of 95 Ma (equivalent to a K-Ar age) implies that this body was intruded during the youngest episode, which is obviously not the case as indicated by the Ar-40/Ar-39 spectrum. In fact, the total fusion ages determined in this study range from 50 Ma to 135 Ma, and there is no means of determining the reliability of these ages without studying the step-heating spectra. To the present time, most of the dating carried out on Arctic volcanics in the Cretaceous, has been done using the conventional K-Ar method, so perhaps many of those samples need to be redated. Although Ar-40/Ar-39 spectra cannot always be interpreted to give correct dates, the ambiguity of the results is generally quite obvious.

7.2. Geological Interpretation

From the data collected, it appears that three of the four major episodes of igneous activity in the Sverdrup Basin are represented by the sills and dykes studied in this project.

Buchanan Lake Sill A was apparently intruded during the Valanginian. This date was obtained from the samples from the sill interior (AX85-217 and AX85-218), with particular emphasis on the biotite age. Biotite retains argon up to temperatures of 300° to 350°C and therefore its thermal history is not easily overprinted. The intrusion of this sill coincided in time and region with the first Cretaceous volcanic episode.

About 15 Ma later, in the late Barremian to early Aptian, Dyke Q/R was intruded. As noted earlier, Dyke Q/R cuts calcite veins within the uppermost sill of the Buchanan Lake Sills. This observation has been taken as confirmation that there was a lapse of time between these two intrusive events. Chilled margins tend to be the most susceptible to thermal overprinting, due to their fine-grained textures (Turner et al, 1966). It is therefore not surprising that sample AX85-215, from the chilled-margin of Sill A, yielded a plateau age almost identical to that of Dyke Q/R (AX85-62), which was emplaced during the episode which caused the thermal

disturbance. The intrusion of this dyke coincided with the second Cretaceous volcanic episode.

The Tropical Ridge basalt flow, which overlies the Hassel Fromation at Lake Hazen on the basin margin, was emplaced during the latter portion of the Cenomanian. Sill #4 of the Star Complex at Piper Pass, also near the basin margin, was intruded at the boundary between the Cenomanian and the Turonian. These two igneous events both coincide with the youngest Cretaceous volcanic episode of the Sverdrup Basin. That episode is thought to be represented in many Late Cretaceous strata in northern Ellesmere Island which have not yet been dated definitely. However, Trettin and Parrish (in prep.) have used the U/Pb zircon method to date the Wooton Intrusion and Hanson Point volcanics to be 92±1 Ma and 88+20/-20 Ma, respectively.

Chapter 8. Conclusions

1a) High-K phases from dyke/sill/flow interiors, if formed soon after the time of emplacement, are best for dating, provided no significant thermal disturbance has occurred which exceeded the argon blocking temperature of the mineral of interest.

b) Whole rock fractions from chilled-margins, containing volcanic glass or another high-K phase (eg. K-feldspar, sericite, biotite), are also good for dating, again provided no significant thermal disturbancehas occurred. This requires rapid cooling as well as the crystallization of high-K phases at the time of cooling.

c) Low-K separates (eg. mafics, plagioclase) have proved to be unreliable for dating by the Ar-40/Ar-30 method, even in apparently undisturbed or mildly disturbed samples.

2a)Tropical Ridge volcanic is probably a flow extruded 92$\pm$2 Ma ago.

b) Star Complex Sill #4 was intruded 91$\pm$2 Ma ago.

c) Buchanan Lake Dyke Q/R was intruded 113$\pm$6 Ma ago.

d) Buchanan Lake Sill A was intruded 126$\pm$2 Ma ago.

3a) Ca/K ratios of particular minerals determined by microprobe analyses do not correlate quantitatively with Ar-37/Ar-39 ratios of

particular heating steps in these samples. This is probably due to dilution or mixing of gases from the outgassing of two or more phases during one heating step.

Bibliography

Balkwill, H.R., "Geology of Amund Ringnes, Cornwall, and Haig-Thomas Islands, District of Franklin", Geol. Surv. Can., Mem. 390, 1983.

Balkwill, H.R., "Evolution of the Sverdrup Basin", American Assoc. Petrol. Geol. Bull., 62, no. 2, 1978, p. 1004-1028.

Berger, G.W., and York D., "Geothermometry from $^{40}Ar/^{39}Ar$ Dating Experiments", Geochim. Cosmochim. Acta, 45, 1981, p. 795-811.

Berger, W., and York, D., "Precision of the $^{40}Ar/^{39}Ar$ Dating Technique", Earth Planet. Sci. Lett., 9, 1970, p. 39-44.

Bottomley, R.J., and Yord, D., "^{40}Ar-^{39}Ar Age Determinations on the Owyhee Basalt of the Columbia Plateau", Earth Plant. Sci. Lett., 31, 1976, p. 75-84.

Brereton, N.R., "A Reappraisal of the $^{40}Ar/^{39}Ar$ Stepwise Degassing Technique", Geophys.. J. R. Astr. Soc., 27, 1972, p. 449-478.

Dallmeyer, R.D., "$^{40}Ar/^{39}Ar$ Dating: Principles, Techniques and Applications in Orogenic Terranes", Lectures in Isotope Geology, Springer-Verlag, 1979, p. 77-104.

Elias, P., "Thermal History of Meguma Terrane: A Study Based on ^{40}Ar-^{39}Ar and Fission Track Dating", unpub. Ph.D. Thesis, Dalhousie University, Halifax, Nova Scotia, 1986, 403 p.

Embry, A.F., et al, unpub. untitled paper, in prep.

Fortier, Y.O., Blackadar, R.G., Glenister, B.F., Greiner, H.R., McLaren, D.J., McMillan, N.J., Norris, A.W., Roots, E.F., Souther, J.G., Thorsteinsson, R., and Tozer, E.T., "Geology of the North-Central Part of the Arctic

Archipelago, Northwest Territories (Operation Franklin)", Geol. Surv. Can., Mem. 320, 1963.

Grist, A., "Low Temperature Geochronology of the South Mountain Batholith, Nova Scotia, Using $^{40}Ar^{*}/^{39}Ar$ and Fission Track Dating Techniques", unpub. Honours Thesis, Dalhousie University, Halifax, Nova Scotia, 1986, 70 p.

Hanes, J.A., "Problems and Progress in the Dating of Precambrian Mafic Dyke Swarms", in Geol. Assoc. Can. Special Paper, "Mafic Dyke Swarms: Intrusion Mechanics, Geodynamic Significance and Global Distribution", in press.

Hanes, J.A., Archibald, D.A., and Lee, J.K.W., "$^{40}Ar/^{39}Ar$ Systematics of Diabase Dykes and their Contact Aureoles in the Kapuskasing Structural Zone and Adjacent Greenstone Belts: Implications for the Tectonothermal Evolution of a Major Archean Crustal Cross-Section in the Canadian Shield", Geochim. Cosmochim. Acta, in press.

Hanes, J.A., York, D., and Hall, C.M., " $^{40}Ar/^{39}Ar$ Geochronological and Electron Microprobe Investigation of an Archean Pyroxenite and its Bearing on Ancient Atmospheric Compositions", Can. J. Earth Sci., 22, 1985, p. 947-958.

Hanes, J.A., and York, D., "A Detailed $^{40}Ar/^{39}Ar$ Age Study of an Abitibi Dike from the Canadian Superior Province", J. Earth Sci., 16, 1978, p. 1060-1070.

Hanson, G.N., $^{40}Ar/^{39}Ar$ Spectrum Ages on Logan Intrusions, a Lower Keweenawan Flow, and Mafic Dikes in Northeastern Minnesota -- Northwestern Ontario", Can. J. Earth Sci., 12, 1975, p. 821-835.

Harrison, T.M., "Some Observations on the Interpretation of $^{40}Ar/^{39}Ar$ Age

Spectra", Isotope Geoscience, 1, 1983, p. 319-338.

Harrison, T.M., and Be, K., "$^{40}Ar/^{39}Ar$ Age Spectrum Analysis of Detrital Microclines from the Southern San Joaquin Basin, California: An Approach to Determining the Thermal Evolution of Sedimentary Basins", Earth Planet. Sci. Lett., 64, 1983, p. 244-256.

Harrison, T.M., Duncan, I., and McDougall, I., "Diffusion of ^{40}Ar in Biotite: Temperature, Pressure and Compositional Effects", Geochim. Cosmochim. Acta, 49, 1985, p. 2461-2468.

Harrison, T.M., and Fitz Gerald, J.D., "Exsolution in Hornblende and its Consequences for $^{40}Ar/^{39}Ar$ Age Spectra and Closure Temperature", Geochim. Cosmochim. Acta, 50, p. 247-253.

Harrison, T.M., and McDougall, I., "The Thermal Significance of Potassium Feldspar K-Ar Ages Inferred from $^{40}Ar/^{39}Ar$ Age Spectrum Results", Geochim. Cosmochim. Acta, 46, 1982, p. 1811-1820.

Hunzicker, J.C., Frey, M., Clauer, N., Dallmeyer, R.D., Friedrichsen, H., Flehmig, W., Hochstrasser, K., Roggwiler, P., and Schwander, H., "The Evolution of Illite to Muscovite: Mineralogical and Isotopic Data from the Glarus Alps, Switzerland", Contrib. Mineral Petrol, 92, 1986, p. 157-180.

Hurford, A.J., and Hammerschmidt, K., "$^{40}Ar/^{39}Ar$ and K/Ar Dating of the Bishop and Fish Canyon Tuffs: Calibration Ages for Fission-Track Dating Standards", Chemical Geology (Isotope Geoscience Section), 58, 1985, p.23-32.

Jackson, K.C., and Halls, H.C., "A Paleomagnetic Study of the Igneous Rocks of the Sverdrup Basin, Canadian Arctic Archipelago", (Abstract), GAC-MAC-CGU, 1983 Joint Meeting Victoria, Program with Abstracts, 8, 84 p.

Jollimore, W., "Analyses of Dyke Swarms Within the Sverdrup Basin, Queen Elizabeth Islands", unpub. Honours Thesis, Dalhousie University, Halifax, Nova Scotia, 1986, 54 p.

Lanphere, M.A., Dalrymple, G.B., "Identification of Excess ^{40}Ar by the $^{40}Ar/^{39}Ar$ Age Spectrum Technique", Earth Planet. Sci. Lett., 32, 1976, p. 141-148.

Larochelle, A., Black, T.F., and Wanless, R.K., "Paleomagnetism of the Isachsen Diabasic Rocks", Nature, 208, no. 5006, 1965.

Leech, A.P., "K/Ar Dates of Basic Intrusive Rocks of the District of Mackenzie, N.W.T.", Can. J. Earth Sci., 3, 1966, p. 389-412.

Makluski, H., "Behaviour of Biotites, Amphiboles, Plagioclases and K-Feldspars in Response to Tectonic Events with the $^{40}Ar/^{39}Ar$ Radiometric Method. Example of Corsican Granite", Geochim. Cosmochim. Acta, 42, 1978, p. 1619-1633.

Mayr, U., Trettin, H.P., and Embry, A.F., "Preliminary Geological Map and Notes, Clements Markham Inlet and Robeson Channel Map Areas, District of Franklin. (NTS 120 E, F, G)", Geol. Surv. Can. Open File 883, 1982a, 40p.

Nassichuck, W.W., and Davies, G.R., "Stratigraphy and Sedimentation of the Otto Fiord Formation", Geol. Surv. Can., Bull. 286, 1980.

Osadetz, K.G., et al, unpub. untitled paper, in prep.

Ozima, M., Kaneoka, I., Yanagisawa, M., "Temperature and Pressure Effects on $^{40}Ar/^{39}Ar$ Systematics", Earth Planet. Sci. Lett., 42,1979, p. 463-472.

Roddick, J.C., "High Precision Intercalibration of ^{40}Ar-^{39}Ar Standards", Geochim. Cosmochim. Acta, 47, 1983, p. 887-898.

Reynolds, P.H., Elias, P., Muecke, G.K., and Grist, A., "Thermal History of the

Southeastern Meguma Zone, Nova Scotia, from an $^{40}Ar/^{39}Ar$--Fission Track Dating Study of Intrusive Rocks", in prep.

Reynolds, P.H., Zentilli, M., and Muecke, G.K., "K-Ar and $^{40}Ar/^{39}Ar$ Geochronology of Granitoid Rocks from Southern Nova Scotia: Its Bearing on the Geological Evolution of the Meguma Zone of the Appalachians", Can. J. Earth Sci., 18, no. 2, 1981, p. 386-394.

Stephenson, R.A., Embry, A.F., Nakiboglu, S.M., and Hastaoglu, M.A., "Rift-Initiated Permian--Early Cretaceous Subsidence of the Sverdrup Basin", unpub. paper presented at the Symposium of Basins of Eastern Canada and Worldwide Analogues, Halifax, Nova Scotia, August 13-15, 1986.

Stevens, R.D., Delabio, R.N., and Lachance, G.R., "Age Determinations and Geological Studies, K-Ar Isotopic Ages, Report 16", Geol. Surv. Can., Paper 82-2, 1982.

Stukas, V., Reynolds, P.H., "$^{40}Ar/^{39}Ar$ Dating of Long Range Dikes, Newfoundland", Earth Planet. Sci. Lett., 22, 1974, p. 256-266.

Trettin, H.P., and Parrish, R., "Late Cretaceous Bimodal Magmatism, Northern Ellesmere Island: Isotopic Age and Origin", Geol. Surv. Can., in prep.

Turner, G., Miller, J.A., Grasty, R.L., "Thermal History of the Bruderheim Meteorite", Earth Planet. Sci. Lett., 1, 1966, p. 155-157.

Turner, G., "Thermal Histories of Meteorites by the ^{39}Ar-^{40}Ar Method", In: Meteoric Research, ed. P.M. Millman, Reidel, 1969, p. 407-417.

Wanless, R.K., Stevens, R.D., Lachance, G.R., and Delabio, R.N., "Age Determinations and Geological Studies, K-Ar Ages, Report 13", Geol. Surv. Can., Paper 77-2, 1977.

Williamson, M-C., "Cretaceous Magmatism in the Western Queen Elizabeth Islands, Arctic Canada", unpub. Progress Report,1984.

Williamson, M-C., "Cretaceous Magmatism in the Western Queen Elizabeth Islands, Arctic Canada", unpub. Progress Report,1985.

York, D., "Cooling Histories from $^{40}Ar/^{39}Ar$ Age Spectra: Implications for Precambrian Plate Tectonics", Ann. Rev. Earth Planet. Sci., 12, 1984, p.383-409.

Zeitler, P.K., and Fitz Gerald, J.D., "Saddle-Shaped $^{40}Ar/^{39}Ar$ Age Spectra from Young, Microstructurally Complex Potassium Feldspars", Geochim. Cosmochim. Acta, 50, 1986, p. 1185-1199.

Appendix A

Photographic Plates

Plate 1. Star Complex, Piper Pass, Ellesmere Island

Dyke/sill complex of basaltic composition which intrudes Permian sandstones of the Trold Fjord Formation. Feeder dykes can be seen merging into sills.

Plate 2. Star Complex, Piper Pass

In the foreground are feeder dykes of basaltic composition cutting sandstones of the Permian Trold Fjord Formation. Sill #4, which was dated (samples EL84-49 and EL84-50) is located in the valley below.

Plate 3. Buchanan Lake, Axel Heiberg Island

Thick sills (up to 50 m) intrude sandstones and shales of the Triassic Blaa Mountain Formation. Note a) the dyke in the section between two thick sills (centre of photograph), b) the slight bleaching of the shales on contact with the sills, and c) the strong vertical jointing of the sills.

Plate 4. Buchanan Lake, Axel Heiberg Island

This view overlooks Sill P, showing Dyke Q/R cutting the sill. The dyke also cuts calcite-filled fractures within the sill. Note a) the irregular nature of the dyke boundary, and b) the blocky jointing of the sill.

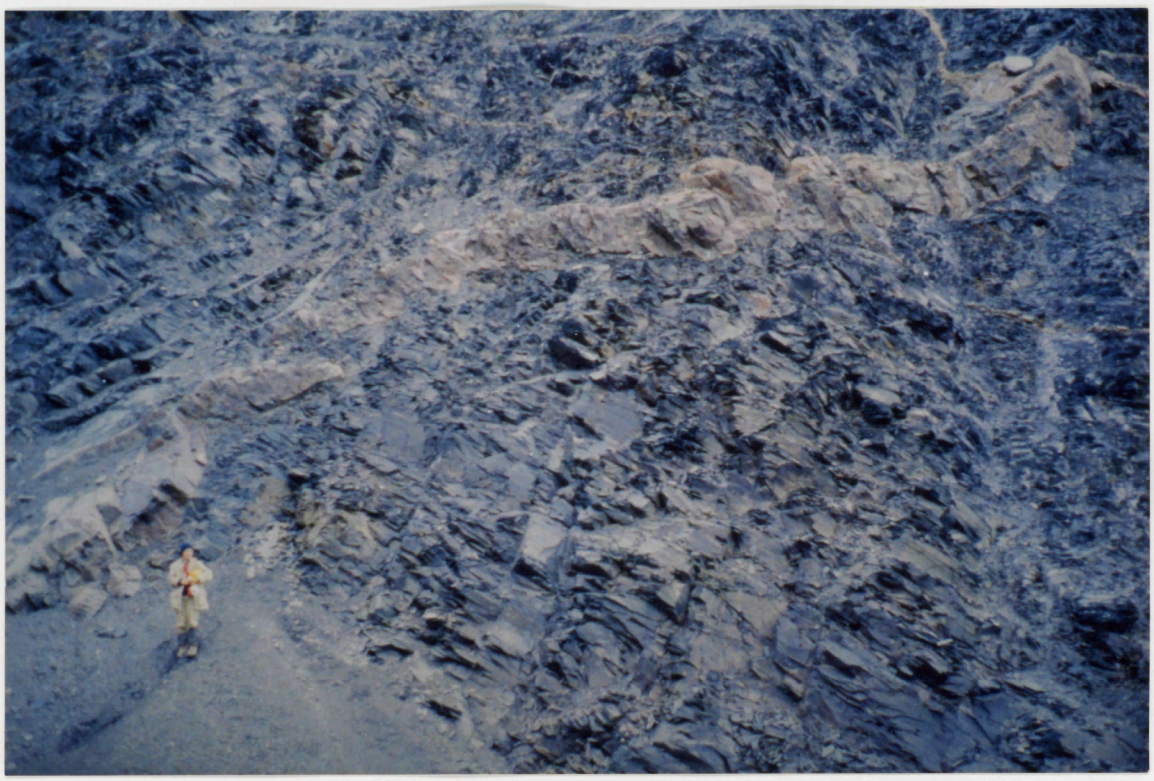

Appendix B

Microprobe Results

Microprobe Analyses

These analyses were carried out on a Jeol 733 electron microprobe. It was operated at 15 KeV and 5 nA using the Tracer Northern ZAF lattice correction method. One standard (Albite) was used to calibrate the microprobe for all of the analyses. An Albite standard analysis follows:

OXIDE	RESULTS WT%
SIO2	69.18
TIO2	0.00
AL2O3	19.91
CR2O3	0.00
FEO	0.00
NIO	0.00
MNO	0.00
MGO	0.00
CAO	0.00
NA2O	10.64
K 2O	0.00
TOTAL=	99.73

EL84-50 PLAGIOCLASE

OXIDE RESULTS		Core	Mid1	Mid2	Rim
	WT%	WT%	WT%	WT%	WT%
SIO2	51.22	51.47	52.25	51.68	51.22
TIO2	0.08	0.09	0.06	0.12	0.15
AL2O3	30.15	29.91	30.11	29.94	30.16
CR2O3	0.00	0.00	0.04	0.00	0.01
FEO	0.54	0.50	0.55	0.42	0.59
NIO	0.00	0.00	0.00	0.00	0.00
MNO	0.00	0.00	0.00	0.00	0.00
MGO	0.06	0.06	0.04	0.10	0.03
CAO	13.50	13.50	13.21	13.43	13.52
NA2O	3.80	3.73	3.60	3.95	3.99
K 2O	0.17	0.25	0.08	0.17	0.16
TOTAL=	99.51	99.51	99.91	99.81	99.83

OXIDE RESULTS					
	WT%	WT%	WT%	WT%	WT%
SIO2	51.33	51.73	51.72	52.70	54.19
TIO2	0.10	0.00	0.12	0.12	0.16
AL2O3	29.73	29.66	29.83	29.46	28.00
CR2O3	0.00	0.06	0.01	0.00	0.00
FEO	0.58	0.56	0.64	0.56	0.63
NIO	0.00	0.00	0.00	0.00	0.00
MNO	0.01	0.00	0.00	0.00	0.00
MGO	0.10	0.05	0.10	0.05	0.00
CAO	13.53	13.26	13.49	12.62	10.58
NA2O	3.81	3.93	3.97	4.23	5.61
K 2O	0.22	0.16	0.18	0.27	0.36
TOTAL=	99.42	99.41	100.05	100.01	99.52

OXIDE RESULTS					
	WT%	WT%	WT%	WT%	WT%
SIO2	51.55	53.00	52.12	51.34	57.35
TIO2	0.10	0.08	0.15	0.10	0.04
AL2O3	29.27	29.59	30.01	30.44	26.00
CR2O3	0.00	0.00	0.05	0.05	0.00
FEO	0.45	0.50	0.55	0.55	0.47
NIO	0.00	0.00	0.00	0.00	0.00
MNO	0.00	0.00	0.00	0.01	0.00
MGO	0.11	0.07	0.12	0.11	0.07
CAO	12.68	12.86	13.40	13.71	8.37
NA2O	4.31	4.08	4.01	3.79	6.07
K 2O	0.25	0.27	0.23	0.17	0.55
TOTAL=	98.72	100.44	100.63	100.27	98.92

EL84-50 GLASS

OXIDE RESULTS					
	WT%	WT%	WT%	WT%	WT%
SIO2	67.94	71.07	67.17	70.85	71.96
TIO2	0.51	0.16	0.59	0.34	0.29
AL2O3	11.90	12.09	14.97	12.11	12.51
CR2O3	0.04	0.03	0.08	0.00	0.02
FEO	3.02	0.16	2.40	0.43	0.22
NIO	0.00	0.00	0.00	0.00	0.00
MNO	0.07	0.07	0.02	0.00	0.02
MGO	0.10	0.00	0.54	0.00	0.00
CAO	0.42	0.47	0.64	0.44	0.33
NA2O	3.57	3.45	3.78	3.79	3.19
K 2O	2.48	2.09	7.31	2.11	4.38
TOTAL=	90.04	89.59	97.50	90.07	92.92

OXIDE RESULTS				
	WT%	WT%	WT%	WT%
SIO2	73.50	69.05	66.80	68.43
TIO2	0.12	0.38	0.39	0.43
AL2O3	11.46	11.73	12.30	12.82
CR2O3	0.00	0.00	0.01	0.00
FEO	0.88	2.14	4.24	1.66
NIO	0.00	0.00	0.00	0.00
MNO	0.00	0.02	0.00	0.00
MGO	0.16	0.21	0.62	0.01
CAO	0.15	0.33	0.35	0.49
NA2O	3.07	3.68	3.68	3.78
K 2O	7.37	2.60	2.52	2.40
TOTAL=	96.69	90.14	90.90	90.02

AX85-62 IDDINGSITE

OXIDE RESULTS				
	WT%	WT%	WT%	WT%
SIO2	48.95	51.09	48.21	46.54
TIO2	0.01	0.01	0.09	0.00
AL2O3	2.36	1.61	2.16	2.51
CR2O3	0.12	0.06	0.03	0.03
FEO	22.76	19.07	23.76	22.37
NIO	0.00	0.00	0.00	0.00
MNO	0.04	0.00	0.00	0.11
MGO	13.85	16.78	12.69	12.70
CAO	0.67	0.44	0.77	0.87
NA2O	0.16	0.05	0.01	0.15
K 2O	0.07	0.05	0.06	0.02
TOTAL=	88.99	89.16	87.79	85.29

AX85-217 PLAGIOCLASE

OXIDE RESULTS		Core	Mid1	Mid2	Rim
	WT%	WT%	WT%	WT%	WT%
SIO2	56.94	53.00	53.88	55.51	53.98
TIO2	0.07	0.07	0.06	0.04	0.07
AL2O3	28.31	29.38	28.81	27.73	27.84
CR2O3	0.00	0.04	0.07	0.00	0.00
FEO	0.57	0.64	0.59	0.64	0.56
NIO	0.00	0.00	0.00	0.00	0.00
MNO	0.00	0.00	0.00	0.00	0.00
MGO	0.01	0.04	0.01	0.02	0.01
CAO	10.63	12.47	11.58	10.17	10.94
NA2O	3.20	4.36	4.90	5.58	5.36
K 2O	0.15	0.20	0.17	0.17	0.22
TOTAL=	99.87	100.20	100.05	99.85	98.98

OXIDE RESULTS					
	WT%	WT%	WT%	WT%	WT%
SIO2	53.07	53.49	52.48	55.88	59.47
TIO2	0.02	0.11	0.11	0.09	0.01
AL2O3	28.57	28.61	29.27	27.69	25.26
CR2O3	0.02	0.00	0.00	0.05	0.05
FEO	0.29	0.20	0.66	0.47	0.13
NIO	0.00	0.00	0.00	0.00	0.00
MNO	0.02	0.00	0.00	0.00	0.00
MGO	0.00	0.01	0.00	0.00	0.00
CAO	11.90	11.78	12.54	9.68	7.31
NA2O	4.56	4.73	4.10	5.82	6.99
K 2O	0.21	0.11	0.15	0.34	0.59
TOTAL=	98.65	99.04	99.29	100.01	99.80

OXIDE RESULTS					
	WT%	WT%	WT%	WT%	WT%
SIO2	52.53	53.58	52.73	54.55	64.73
TIO2	0.12	0.05	0.05	0.11	0.00
AL2O3	29.28	28.59	29.03	28.25	21.89
CR2O3	0.00	0.00	0.00	0.01	0.00
FEO	0.60	0.45	0.62	0.51	0.16
NIO	0.00	0.00	0.00	0.00	0.00
MNO	0.00	0.00	0.00	0.00	0.00
MGO	0.00	0.00	0.03	0.01	0.00
CAO	12.53	11.45	12.30	10.88	3.15
NA2O	4.49	4.88	4.45	5.28	9.22
K 2O	0.08	0.22	0.11	0.27	1.06
TOTAL=	99.63	99.22	99.32	99.86	100.20

AX85-217 HORNBLENDE

OXIDE RESULTS					
	WT%	WT%	WT%	WT%	WT%
SIO2	41.99	46.25	41.99	48.89	43.25
TIO2	0.14	0.40	0.14	0.96	0.10
AL2O3	6.11	3.54	6.25	1.74	5.83
CR2O3	0.11	0.07	0.11	0.00	0.09
FEO	21.93	17.20	22.32	11.46	21.73
NIO	0.00	0.00	0.00	0.00	0.00
MNO	0.07	0.28	0.21	0.16	0.19
MGO	12.03	11.49	11.47	11.49	12.14
CAO	8.12	16.46	9.14	17.68	9.35
NA2O	0.22	0.18	0.28	0.34	0.23
K 2O	0.09	0.04	0.19	0.01	0.10
TOTAL=	90.81	95.91	92.09	92.73	92.99

AX85-217 CLINOPYROXENE (AUGITE)

OXIDE RESULTS				
	WT%	WT%	WT%	WT%
SIO2	49.78	50.77	50.28	50.63
TIO2	0.86	0.82	0.88	0.88
AL2O3	1.97	2.44	2.03	2.25
CR2O3	0.00	0.11	0.05	0.03
FEO	12.11	10.32	12.72	11.34
NIO	0.00	0.00	0.00	0.00
MNO	0.26	0.23	0.27	0.21
MGO	14.63	15.39	14.20	14.78
CAO	17.97	18.33	17.60	18.46
NA2O	0.36	0.34	0.25	0.32
K 2O	0.00	0.00	0.00	0.00
TOTAL=	97.93	98.73	98.28	98.90

AX85-218 PLAGIOCLASE

OXIDE RESULTS		Core	Mid1	Mid2	Rim
	WT%	WT%	WT%	WT%	WT%
SIO2	55.12	55.16	56.81	62.42	64.20
TIO2	0.03	0.06	0.03	0.00	0.03
AL2O3	28.14	28.26	27.56	23.52	22.67
CR2O3	0.00	0.04	0.00	0.00	0.00
FEO	0.43	0.44	0.26	0.23	0.00
NIO	0.00	0.00	0.00	0.00	0.00
MNO	0.00	0.12	0.00	0.00	0.03
MGO	0.01	0.01	0.00	0.00	0.00
CAO	10.35	10.88	9.57	5.09	3.62
NA2O	5.68	5.69	6.19	7.99	8.81
K 2O	0.29	0.29	0.27	0.75	1.18
TOTAL=	100.05	100.95	100.68	99.98	100.54

OXIDE RESULTS					
	WT%	WT%	WT%	WT%	WT%
SIO2	56.38	56.42	57.22	58.44	61.76
TIO2	0.00	0.00	0.02	0.06	0.00
AL2O3	27.01	26.78	26.51	25.94	23.70
CR2O3	0.02	0.01	0.01	0.00	0.04
FEO	0.36	0.36	0.25	0.16	0.05
NIO	0.00	0.00	0.00	0.00	0.00
MNO	0.00	0.00	0.00	0.00	0.00
MGO	0.00	0.00	0.00	0.00	0.00
CAO	9.93	9.52	9.02	8.26	5.64
NA2O	6.06	6.27	6.44	6.79	7.74
K 2O	0.34	0.28	0.39	0.42	0.63
TOTAL=	100.10	99.64	99.85	100.08	99.55

OXIDE RESULTS						
	WT%	WT%	WT%	WT%	WT%	WT%
SIO2	54.60	54.44	54.79	56.52	63.70	62.26
TIO2	0.12	0.00	0.06	0.01	0.00	0.04
AL2O3	27.95	27.10	27.61	26.30	22.34	23.13
CR2O3	0.00	0.02	0.00	0.01	0.00	0.03
FEO	0.21	0.51	0.43	0.23	0.10	0.08
NIO	0.00	0.00	0.00	0.00	0.00	0.00
MNO	0.03	0.01	0.00	0.03	0.00	0.00
MGO	0.03	0.04	0.05	0.00	0.00	0.00
CAO	11.09	10.62	11.30	9.45	4.27	4.90
NA2O	4.31	5.35	5.41	5.83	8.62	8.21
K 2O	0.19	0.25	0.23	0.30	0.96	0.87
TOTAL=	98.53	98.33	99.87	98.68	100.00	99.52

AX85-218 K-FELDSPAR (OLIGOCLASE)

OXIDE RESULTS

	WT%	WT%	WT%	WT%
SIO2	66.21	66.34	65.50	66.25
TIO2	0.04	0.04	0.06	0.00
AL2O3	18.99	19.03	18.84	19.20
CR2O3	0.04	0.00	0.01	0.05
FEO	0.04	0.00	0.00	0.12
NIO	0.00	0.00	0.00	0.00
MNO	0.00	0.10	0.00	0.00
MGO	0.00	0.00	0.00	0.00
CAO	0.20	0.39	0.05	0.12
NA2O	4.86	5.73	2.87	4.57
K 2O	9.69	8.26	11.73	10.02
TOTAL=	100.06	99.88	99.06	100.33

AX85-218 BIOTITE

OXIDE RESULTS

	WT%	WT%	WT%
SIO2	35.39	35.94	34.20
TIO2	3.57	3.31	3.56
AL2O3	12.09	12.00	12.33
CR2O3	0.01	0.13	0.13
FEO	30.54	29.68	33.29
NIO	0.00	0.00	0.00
MNO	0.06	0.16	0.12
MGO	5.01	5.28	2.38
CAO	0.00	0.07	0.08
NA2O	0.34	0.49	0.34
K 2O	8.67	8.76	8.78
TOTAL=	95.68	95.80	95.21